

**Design of a Power Electronics Based Diesel Engine Generator Emulator for Study of  
Microgrid Related Applications**

Hesam Akbarian

A Thesis

in

The Department

of

Electrical and Computer Engineering

Presented in Partial Fulfillment of the Requirements

for the Degree of Master of Applied Science at

Concordia University

Montreal, Quebec, Canada

September 2015

© Hesam Akbarian, 2015

**CONCORDIA UNIVERSITY**  
**SCHOOL OF GRADUATE STUDIES**

This is to certify that the thesis prepared

By: **Hesam Akbarian**

Entitled: **Design of a Power Electronics Based Diesel Engine Generator Emulator  
for Study of Microgrid Related Applications**

and submitted in partial fulfillment of the requirements for the degree of

**Master of Applied Science**

complies with the regulations of the University and meets the accepted standards with respect to originality and quality.

Signed by the final Examining Committee:

_____	Chair
Dr. M. O. Ahmad	
_____	Supervisor
Dr. P. Pillay	
_____	Co-supervisor
Dr. L. A. Lopes	
_____	Examiner
Dr. B. Bhat (MIE)	
_____	Examiner
Dr. M. Z. Kabir	

Approved by \_\_\_\_\_

Dr. W. E. Lynch  
Chair Department of Electrical and Computer Engineering

September 14-2015

\_\_\_\_\_  
Dr. Amir Asif  
Dean, Faculty of Engineering and  
Computer Science

## **ABSTRACT**

### **Design of a Power Electronics Based Diesel Engine Generator Emulator for Study of Microgrid Related Applications**

**Hesam Akbarian**

In the following thesis, design and implementation of an emulator is provided to emulate the parallel operation of a hybrid diesel engine generator (GENSET) and hydrokinetic energy conversion system (HKECS) in a microgrid with the aim of improvement in overall performance of the genset in terms of fuel consumption, emission and efficiency. The mechanical and electrical parts of a typical genset are modeled mathematically in a digital controller (ds-1103, dSpace) and the model is fed to a current and voltage controlled voltage source inverter (VSI) which is designed for the emulation of the generator output voltage to produce the same output power characteristics as in a real diesel engine generator. Output available power of a second source (only steady state behaviour of a HKECS) is emulated using a current controlled VSI (CCVSI); which is fed by reference signals determined by the available power flow of the water. In addition, a novel method for combination of the genset and HKECS is proposed to enforce the genset to operate in the least brake specific fuel consumption (BSFC), most efficient or less emission operating points. Since no dedicated physical communication channel is desirable and generally does not exist in real applications, yet there is a demand to communicate between two sources to keep one in a particular operating point,

a modified droop control scheme is defined to communicate indirectly. A detailed analysis show that efficiency, emission and fuel consumption are significantly improved in comparison with conventional methods. For experimental validation, the control algorithm is implemented in dSpace using the DS-1103 controller. The experimental results confirm improvements in fuel consumption for a specific BSFC curve to 1 *gr* in 10 seconds for a load of  $P=1200$  W by engaging the proposed method.

## **ACKNOWLEDGMENT**

My deepest gratitude to cause of my consciousness who shaped events intelligently and effected my friends and enemies to probably improve and promote me and some others.

Immeasurable appreciations and respect goes to my supervisor professor P. Pillay who honestly believed, accepted, and reflected my capacity into many academic achievements in a short time and gave me the chance to pursue the path that I was eager; and my co-supervisor Professor L. Lopes for his invaluable and effective technical and academic supports during my research and publications.

I would like to thank the government of Canada, for permitting and facilitating my studying and living abroad.

# TABLE OF CONTENTS

<b>ABSTRACT</b> .....	iii
<b>ACKNOWLEDGMENT</b> .....	v
<b>LIST OF FIGURES</b> .....	x
<b>LIST OF TABLES</b> .....	xiii
<b>LIST OF ABBREVIATIONS</b> .....	xiv
<b>LIST OF MAIN SYMBOLS</b> .....	xv
Chapter 1. Introduction.....	1
1.1. General Introduction.....	1
1.2. Microgrid-an Overview.....	2
1.3. Diesel Engine Generator set (Genset).....	3
1.3.1. Automatic Voltage Regulator (AVR).....	4
1.3.2. Speed Governor.....	4
1.3.3. Isochronous Mode of Operation.....	4
1.3.4. Frequency-Droop Controlled Mode of Operation (Active Power Control).....	5
1.3.5. Voltage-Droop Control (Reactive Power Control).....	7
1.4. HKECS.....	8
1.5. Main Contributions.....	9
1.6. Publications:.....	9
1.6.1. Journal:.....	9
1.6.2. Conference paper:.....	9
1.7. Scope of the Thesis.....	10
1.8. Outline of the Thesis.....	10
Chapter 2. Emulation of the Diesel Engine Generator.....	12
2.1. Introduction.....	12
2.2. Modeling of the Diesel Engine Generator.....	13
2.2.1. ICE Model.....	14
2.2.2. Flexible Coupling Shaft Model.....	14
2.2.3. Synchronous Generator Model.....	15

2.2.4. Speed Governor .....	17
2.2.5. Automatic Voltage Regulator .....	17
2.3. Current and Voltage Controlled VSI .....	18
2.4. Droop Controller.....	20
2.5. Experimental Implementation and Validation .....	21
2.5.1. Individual Diesel Genset Experimental Test.....	22
2.6. Summary.....	28
2.7. Conclusions .....	29
2.8. Contributions .....	29
Chapter 3. BSFC, Emission and Efficiency Versus Power in an ICE .....	30
3.1. Introduction .....	30
3.2. BSFC .....	30
3.3. Fuel Efficiency versus Power .....	32
3.4. ICE Efficiency versus Power .....	32
3.5. Emission versus Power .....	34
3.6. Fuel Consumption Cost during the Operation .....	35
3.7. Summary.....	36
Chapter 4. HKECS Steady State Output Power Emulation.....	37
4.1. Introduction .....	37
4.2. Predicting the Available Power and Torque .....	38
4.3. Configuration of a HKECS.....	39
4.4. Power delivery to the Load.....	39
4.4.1. Decoupled Control of the $PQ$ .....	40
4.4.2. Current Controlled VSI.....	41
4.5. Experimental Implementation and Validation .....	42
4.5.1. Coupled $PQ$ control of the HKECS .....	42
4.5.2. Decoupled $PQ$ control of the HKECS .....	43

4.6. Summary.....	46
4.7. Conclusion.....	46
4.8. Contributions .....	46
Chapter 5. Parallel Operation of the Genset and HKECS .....	47
5.1. Introduction .....	47
5.2. Considerations for Parallel operation .....	48
5.2.1. Synchronization .....	48
5.2.2. Load Sharing.....	49
5.2.3. Protection.....	49
5.3. Experimental Validations .....	50
5.4. Summary.....	53
5.5. Conclusion.....	53
Chapter 6. IOP tracking of the genset using HKECS .....	54
6.1. Introduction .....	54
6.2. General Description of the Method .....	54
6.3. A modified Droop Control Scheme for IOP Tracking of the Genset .....	55
6.3.1. The Real Case .....	57
6.4. Compensation of the Power.....	59
6.5. Experimental Validations .....	60
6.5.1. Linear Droop.....	60
6.5.2. Modified Droop .....	64
6.6. Summary.....	66
6.7. Conclusions .....	66
6.8. Contributions .....	66
Chapter 7. Summary and Conclusion .....	67
7.1. Summary.....	67
7.2. Conclusion.....	68

7.3. Future Works .....	68
APPENDIX A .....	69
APPENDIX B .....	72
REFERENCES .....	74

## LIST OF FIGURES

Figure 1-1: Typical structure of a microgrid [14] .....	2
Figure 1-2: Typical structure of a diesel genset .....	4
Figure 1-3: Isochronous controlled output frequency vs. power [15]. .....	5
Figure 1-4: (a) Synchronous Generator connected to the infinite bus (b) Effect of increased torque on the output power [17]. .....	6
Figure 1-5: Droop controlled output frequency vs. power [15]. .....	7
Figure 1-6: Effect of excitation (output voltage amplitude) on the output power (a) Increased excitation, (b) Decreased excitation [17]. .....	7
Figure 1-7: Typical structure of a HKECS .....	8
Figure 2-1: A commercial genset .....	12
Figure 2-2: Connections and components in a commercial genset. Modelled components are marked with the red circle. ....	13
Figure 2-3: Diesel Engine Generator incorporated in a microgrid. ....	13
Figure 2-4: Diesel engine and generator mechanical models. ....	15
Figure. 2-5: SG equivalent model in dq-frame. ....	16
Figure. 2-6: PI controller for speed governor. ....	17
Figure. 2-7: Automatic voltage regulator for the diesel engine generator. ....	18
Figure. 2-8: VSI block diagram [24]. ....	18
Figure. 2-9: (a) Voltage and (b) current controller loops block diagrams [24]. ....	20
Figure. 2-10: Speed-Droop governor. ....	21
Figure. 2-11: Implemented hardware setup of the Emulator under the test. ....	22
Figure. 2-12: (a) Measured output voltage in the abc frame (Scale=4.7:1); (b) X-Y graph to verify the quality of output voltage (Scale=4.7:1). ....	23
Figure. 2-13: Measured output signal of the Emulator in response to a step load change (a) Measured output RMS voltage (Scale=20:1) (b) Actual shaft RPM of the SG (Scale=600/ $\pi$ :1). ....	23
Figure. 2-14: Response to a step load increase in isochronous speed governor [18]. ....	24
Figure. 2-15: Transient response of the emulator for different values of droop studied in [15]. ....	25
Figure. 2-16. Output frequency change during a step load change from 1 kW to 3.5 kW for 1% droop. (Power scale: 350:1, Frequency scale: 81/4 $\pi$ :1). ....	26
Figure. 2-17. The droop line for a 1% droop. ....	26
Figure. 2-18. The response to a step load increase in a droop controlled speed governor studied in [18]. (a) Frequency power droop (b) Response to step load power. ....	27

Figure. 2-19. Output frequency change during a load step change from 1 kW to 3.5 kW for (a) 3% and (b) 5% droop. (Power scale: 350:1, Frequency scale: $81/4\pi:1$ ).-----	28
Figure. 3-1. Quadratic and linear approximations for BSFC versus Power dependency for a sample ICE [28].-----	31
Figure. 3-2. Example ICE efficiency model. The high efficient region is highlighted by the shaded green cap of the 3D model [29].-----	33
Figure. 3-3. Efficiency versus power in three different gensets studied in [1].-----	33
Figure. 3-4. Sample emission characteristic which is studied in [30].-----	35
Figure. 4-1. Wave energy resource estimation [31].-----	37
Figure. 4-2. A typical structure of the HKECS in parallel with a genset.-----	39
Figure. 4-3. A grid tied VSI.-----	40
Figure. 4-4. Power controller of the VSI; $id$ and $iq$ to decouple $PQ$ .-----	41
Figure. 4-5. CCVSI topology.-----	42
Figure 4-6- From Top to Bottom: Generator output active power (Scale 1:350); HKECS output voltage level (scale 1:100); Generator output reactive power (Scale 1:350); HK source output voltage phase difference from genset(scale 1:36);-----	43
Figure. 4-7. Decoupled $PQ$ sharing between genset and HKECS for a 2% frequency droop (a) HKECS output power (b) Genset output active power (c) HKECS output reactive power (d) genset output reactive power (e) Genset shaft frequency-there is an offset of -0.062V in the frequency curve. (Power scale: 350:1, Frequency scale: $20/\pi:1$ ).-----	45
Figure. 5-1. Parallel placement of generators in a power generation utility -----	47
Figure. 5-2. Synchronization stages for two signals-----	48
Figure. 5-3. Output power sharing and frequency of the parallel operation of the genset with a step power generation of a HKECS for 1% droop ( $f_{max} = 61 \text{ Hz}$ , $P_{max} = 5 \text{ kW}$ ). (a) Genset output power (b) HKECS generated power (c) Load power (d) Genset shaft frequency. (Power scale: 350:1, Frequency scale: $20/\pi:1$ ).-----	51
Figure. 5-4. Output power sharing and frequency of the parallel operation of the genset and a HKECS with a power profile of a power plant in Point Evans, for 2% droop ( $f_{max} = 61 \text{ Hz}$ , $P_{max} = 5 \text{ kW}$ ). (a) Genset output power (b) HK source generated power (c) Load power (d) Genset shaft frequency. (Power scale: 350:1, Frequency scale: $20/\pi:1$ ).-----	52
Figure. 6-1. Direct operating point mapping to the frequency-----	56
Figure. 6-2. Linear droop scheme for a genset to reflect IOP (BSFC in this case) in frequency (i.e. to map the BSFC into the power)-the base frequency of 60 Hz happens at IOP in a particular genset.-	57

Figure. 6-3. Linear droop scheme for a genset to reflect IOP (BSFC in this case) in frequency- a case in which the IOP is not happening at the base frequency; Droop line is shifted to force $f_{IOP} = f_{base}$ .	57
Figure. 6-4. A sample modified droop line with 40% ( $p = 0.4$ ) effect of normalized BSFC curve to reflect the BSFC in the frequency.	59
Figure. 6-5. Frequency control of the grid through power delivery .	60
Figure. 6-6. Enforcing genset to the IOP using linear droop control scheme by HKECS. (a) The genset output power (b) Scaled BSFC of the genset in Figure. 3-1 (c) Bus frequency with a linear 3% droop (d) The HKECS output power (Power scale: 350:1, Frequency scale: $20/\pi$ :1, BSFC scale: 80:1).	61
Figure. 6-7. Enforcing genset to the IOP using modified droop control scheme by HKECS. (a) The genset output power (Power scale: 350:1) (b) Scaled BSFC of the genset in Figure. 3-1 (BSFC scale: 80:1) (c) Bus frequency modified droop based on BSFC (Frequency scale: $20/\pi$ :1) (d) The HKECS output power (Power scale: 350:1).	64
Figure. A-7-1. Schematic diagram of a grid connected VSI.	69
Figure. A-7-2. Type-2 PI controller [35].	70
Figure. A-7-3. Schematic diagram of a grid connected VSI [35].	71

## LIST OF TABLES

TABLE I-SPEED GOVERNOR AND AVR CONTROLLER SET PARAMETERS .....	72
TABLE II-VSI CONTROLLER SET PARAMETERS (5 kVA, 110 V, 60 Hz) .....	72
TABLE III-CCVSI CONTROLLER SET PARAMETERS (5 kVA, 110 V, 60 Hz).....	72
TABLE IV- <i>PQ</i> CONTROLLER SET PARAMETERS .....	72
TABLE V-FREQUENCY COMPENSATOR CONTROLLER SET PARAMETERS .....	73
TABLE VI-DIESEL ENGINE PARAMETERS .....	73
TABLE VII-SYNCHRONOUS MACHINE PARAMETERS.....	73

## LIST OF ABBREVIATIONS

Genset	Diesel Engine Generator set
HKECS	Hydrokinetic Energy Conversion System
VSI	Voltage Source Inverter
CCVSI	Current Controlled Voltage Source Inverter
SFC	Specific Fuel Consumption
BSFC	Brake Specific Fuel Consumption
AVR	Automatic Voltage Regulator
HEV	Hybrid Electric Vehicle
DER	Distributed Energy Resources
ICE	Internal Combustion Engine
SG	Synchronous Generator
LPF	Low Pass Filter
ESS	Energy Storage System

## LIST OF MAIN SYMBOLS

$E_t$	Terminal Voltage
$V_B$	Bus (Grid) Voltage
$V_R$	Resultant Voltage
$I_a$	Phase Current
$p$	Derivative Function
$i_d$	d-axis Component of the Current
$i_q$	Q-axis Component of the Current
$v_d$	d-axis Component of the Voltage
$v_q$	Q-axis Component of the Voltage
$f_{IOP}$	Frequency at which the IOP Happens
$P_{IOP}$	Power at which the IOP Happens
$f_{min}$	Minimum Frequency
$f_{NL}$	Genset No-Load Frequency
$P_{full}$	Full Loaded Power
P	Active Power
Q	Reactive Power
PQ	Active and Reactive Powers
$\emptyset$	Terminal and grid Voltages angle difference
X	Coupling impedance

### 1.1. GENERAL INTRODUCTION

Diesel engine power generators are being used as the main power generation unit in remote areas with low population density where the wired electricity transmission is not feasible due to the geographic obstacles or economic justifications. The emission, fuel cost and its transportation which in some rural areas cost 1 litre to transfer 1 litre of fuel are the main issues [1]. Therefore it is desirable to incorporate (hybrid) distributed renewable sources (DER) with diesel generators in those areas which could also be considered as a microgrid. Using diverse distributed energy sources also increase overall reliability of the power generation.

Study of the distributed power generation is expanding rapidly and having access to the real power generators for studying the concepts and to improve power generation quality and consumption in different aspects including emission, efficiency and cost for electricity generation is becoming more of interest [2-3]. Due to the diverse nature of different energy resources, it is challenging and costly to have access to all the different power generators in research laboratories where those studies are to be conducted [4]. One way to overcome those limitations is employing emulators consisting of inverters as part of the system to produce the same output voltage characteristics as in real generators [5]. Many works are done to emulate different energy power generator plants such as wind and hydrokinetic, in terms of rotating and static emulation [6, 8]. However, there are a few works done to emulate the genset, which forms the microgrid in real applications and also are being employed during peak power demand or the power recession as in [7, 9].

The efficiency, emission and BSFC of the internal combustion engines (ICE)-which are vastly used in gensets [2, 5, and 7] - depend on the output power of the genset [10-12]. During the power sharing with various energy resources such as HKECS, genset do not

necessarily work in the best operating point. As proposed in this thesis one can set and track the best operating point of the genset using other DERs as a compensator.

Since the VSI unit is common between different types of generator emulators, and only the type of prime mover, generator and control strategy changes; (and since the current emulator is not designed with only a solid hardware setup and controllers are running in software packages) the emulator configuration is flexible, making it compatible to other applications with the least possible change. The emulator is developed in dSpace using the DS-1103 controller based on a commercial diesel engine generator. To have a better understanding of the parallel operation (as in real applications in microgrids), the same emulator is reconfigured with a CCVSI to be used as HKECS in parallel with diesel engine in island mode. In the following, relevant concepts and systems are explained.

## 1.2. MICROGRID-AN OVERVIEW

Microgrid is a cluster of microsources and loads which are considered as a controllable system that produce both power and heat [13]. DERs are often incorporated in microgrids as is shown in Figure 1-1.

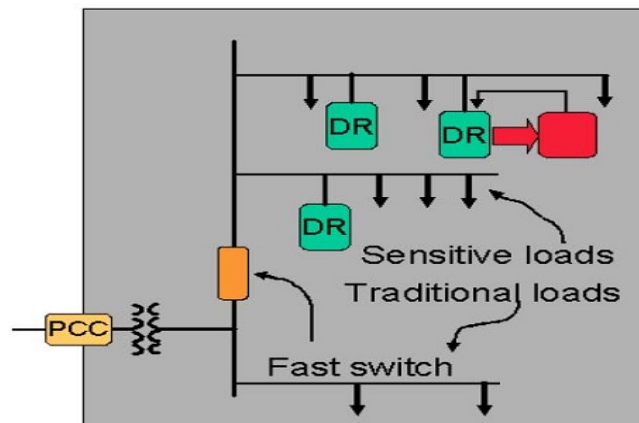


Figure 1-1: Typical structure of a microgrid [14]

A Microgrid has two operating modes, grid connected and islanding mode which are controlled by the main fast-switch breaker. In a microgrid, typically there is no communication channel and power sharing happens through the frequency droop control.

The major features of the Microgrid are [14]:

1. Peer-to-peer environment
2. No explicit communications system
3. Plug-and-play
4. Scalable system
5. CHP to improve efficiency
6. Smooth transfer between island and grid-connected

### **1.3. DIESEL ENGINE GENERATOR SET (GENSET)**

A diesel genset consists of an internal combustion engine (ICE) and a synchronous generator coupled on the same shaft. Such systems are widely used as backup or emergency power in commercial as well as industrial installations. Diesel gensets are also heavily used in remote locations where it is impractical or prohibitively expensive to connect to utility power. Diesel gensets used in prime and continuous power applications are typically designed to operate at higher efficiencies since, in the long run, the fuel costs will dominate the initial capital costs. The generator in the genset is typically either a permanent magnet or a wound-field synchronous machine. In case of a permanent magnet generator, the front end consists of a rectifier and a voltage-source converter to provide the necessary AC voltage at the desired frequency. The presence of a switched controlled power electronics front end increases the overall cost of the system and decreases its fault tolerance. The presence of the inverter enables non-synchronous operation of the engine which makes increased power density and higher efficiency [14].

Figure 1-2 shows structure of a typical diesel genset.

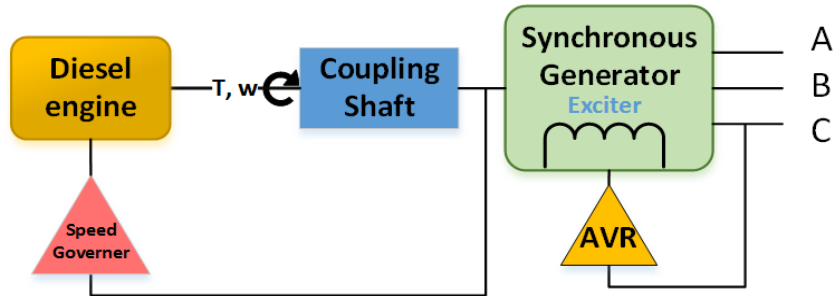


Figure 1-2: Typical structure of a diesel genset

### 1.3.1. Automatic Voltage Regulator (AVR)

The AVR is a controller to regulate and keep the output voltage amplitude of the generator constant. AVR consists of a bridge rectifier connected to the output winding of the Synchronous Generator (SG) to detect available output voltage amplitude of the SG, and a variable DC supply to adjust the exciting current to control the output voltage amplitude using (-typically) a PI controller. This is to keep the output voltage constant while the load or speed of the rotor shaft changes.

### 1.3.2. Speed Governor

The speed governor also is based on a PI controller to keep the rotor shaft speed constant. Speed governor measures the rotor shaft speed and controls the torque applied to the rotor of the generator through controlling the fuel injector valve of the ICE, which is connected to the rotor via a coupling shaft.

### 1.3.3. Isochronous Mode of Operation

In the isochronous mode of operation, the shaft speed (hence the output frequency) is a constant value, and after any turbulences, if the output frequency experiences any transient changes (because of the inertia which is connected to the shaft, etc.) the controller brings the frequency back to its reference value. In contrast to the droop controlled mode, in isochronous mode the reference shaft speed is constant and does not vary according to the output power. Since the output frequency is a fixed value, no

additional controller is required and the governor speed controller could be used with a fixed constant reference speed. The simplest speed governor would be the integral of the speed error that drives the speed to its reference value hence also called integral speed governor. Isochronous mode is used when no more than one generator supplies the load.

Figure 1-3 shows an isochronous controller behaviour. In Figure 1-3 (a) one can see that the reference frequency is independent of the output power. In Figure 1-3 (b) the settling frequency returns back to the reference value after a load turbulence.

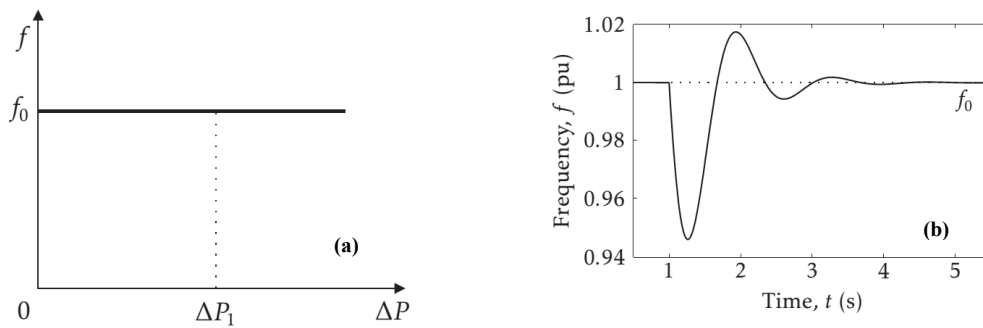


**Figure 1-3: Isochronous controlled output frequency vs. power [15].**

#### 1.3.4. Frequency-Droop Controlled Mode of Operation (Active Power Control)

Changing the generator input mechanical power, so that the rotor phase leads or lags the grid voltage phase, the true power output of the generator changes. Consequently the active power can be controlled [17].

Figure 1-4 (b) illustrates effect of phase (input mechanical power) on output power delivery for the circuit shown in Figure 1-4 (a) which can be represented as:

$$P = 3 \times E_t \times I_a \cos \phi \quad (1.1)$$

or can be represented as:

$$P = 3 \times \frac{E_t \times V_B}{X} \sin \sigma \quad (1.2)$$

where  $\sigma$  is the phase difference between two sources,  $E_t$  is the genset terminal voltage,  $V_B$  is the bus voltage,  $I_a$  is the load current and  $X$  is the coupling impedance.

Equation (1.2) shows when  $E_t = V_B$  and only phase of the two voltages changes (by changing the generator input torque) delivered power can change.

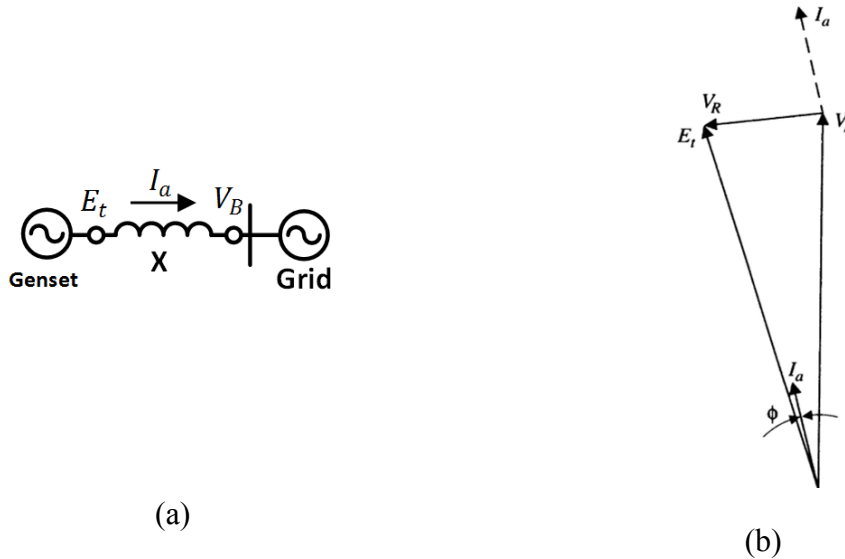


**Figure 1-4: (a) Synchronous Generator connected to the infinite bus (b) Effect of increased torque on the output power [17].**

For parallel operation of more than one generator, the output frequency of each power generation unit are defined to vary according to its output power to facilitate the load estimation and sharing between different generators. Different droop characteristics could be defined for different sources according to the power capacity.

Based on the percentage of the droop, the shaft reference speed of the governor changed linearly with respect to the output power.

Figure 1-5 shows a sample droop controlled genset frequency. In contrast to the Figure 1-3, Figure 1-5 (a) demonstrates dependency of the reference frequency on the delivered power; Figure 1-5 (b) shows how the settling frequency is changed by a step load change.

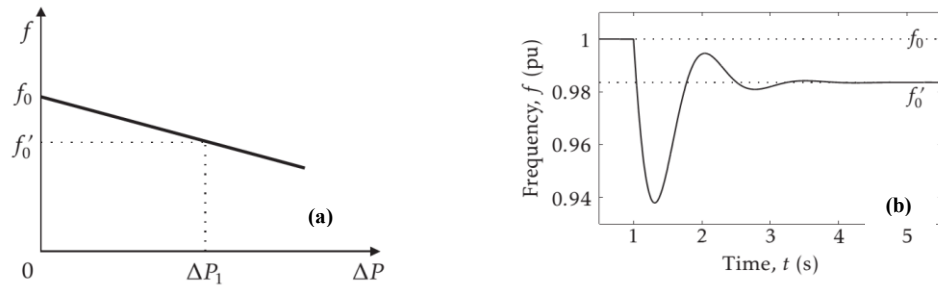


**Figure 1-5: Droop controlled output frequency vs. power [15].**

For two or more generators, the frequency for all of them would be the same thus the active power will be shared based on the droop slope and base frequency [16, 18].

### 1.3.5. Voltage-Droop Control (Reactive Power Control)

Flow of the reactive power could be controlled with the output voltage amplitude using AVR. If the genset output voltage amplitude in Figure 1-4 (a) changes, the resultant voltage across  $x$  ( $V_R$ ) and thus output current make a change in phase with respect to the terminal voltage, so the reactive power could be controlled as could be concluded in Figure 1-6 [17].

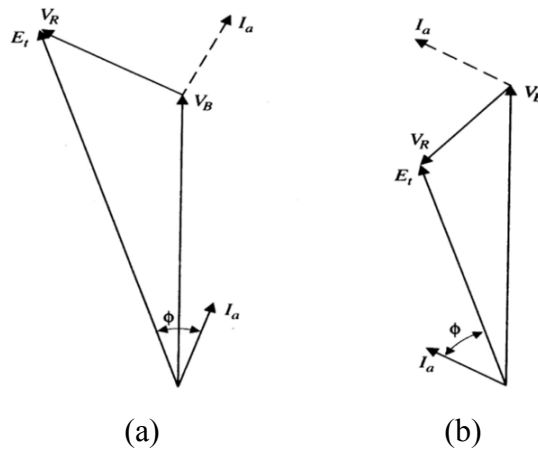


**Figure 1-6: Effect of excitation (output voltage amplitude) on the output power (a) Increased excitation, (b) Decreased excitation [17].**

Figure 1-6 (b) shows effect of increasing the excitation current without further increase in the mechanical input power. As can be seen, when  $E_t$  is increased,  $V_R$  is increased and the angle by which  $I_a$  lags  $V_B$  is increased, that is the power factor is more lagging.

To summarize, a change in phase between  $E_t$  and  $V_B$  changes  $I_a$  amplitude which causes a change in the active power; and a change in the magnitude of the  $E_t$  changes phase of the  $I_a$  which then controls the reactive power.

In another analogy, the power output of the alternator is controlled by the angular movement of the rotor, which is by changing the torque output of the prime mover. The power factor (and consequently the reactive power) is controlled by the rotor excitation, becoming more lagging as the excitation current is increased and more leading when the excitation current is reduced [17]. In other words, the generator tends to supply  $Q$  when over excited and absorb  $Q$  when under excited.

Although active ( $P$ ) and reactive ( $Q$ ) powers can be controlled with the explained methods, however they are coupled together and controlling one affects the other. It will be shown how to decouple  $P$  and  $Q$  using dq-frame theory.

#### 1.4. HKECS

HKECSs which convert the flowing water energy into electrical, are fundamentally similar to wind turbine energy generation principle and are being used in remote areas. HKECS is more reliable than the wind because of the continuity in the flow of the water.

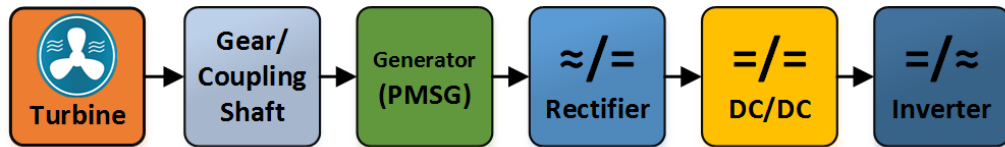


Figure 1-7: Typical structure of a HKECS

## 1.5. MAIN CONTRIBUTIONS

Following are the main contributions in the thesis:

1. A novel methods to enforce the genset to operate in the ideal operating point (IOP) which could be defined based on the minimum BSFC, maximum efficiency or minimum emission. IOP tracking based on the minimum BSFC is studied in the thesis. The method does not require additional communication channel and detects the operating point based on the frequency behaviour.
2. A new method to detect BSFC curve of the genset without using an extra communication channel using droop control method.
3. A generic  $PQ$  decoupling block is proposed which decouples  $P$  and  $Q$  works even if  $v_q \neq 0$ .
4. Compensation/control of the decoupled  $P$  and  $Q$  using a CCVSI.

## 1.6. PUBLICATIONS:

### 1.6.1. Journal:

1. H. Akbarian, P. Pillay, L. Lopes “*Emulation of the Diesel Engine Generator in a Microgrid: A Novel Method to Enforce the Genset to Operate Ideally-A Case with Least Fuel Consumption per Unit Output Power*” to be submitted in the Energy Conversion Transaction on, IEEE.
2. H. Akbarian, P. Pillay “*Induction Machine Parameters Measurement through Processing Its Transient Current Response to a DC Step Voltage*” submitted in the Energy Conversion Transaction on, IEEE.

### 1.6.2. Conference paper:

1. H. Akbarian, P. Pillay, L. Lopes, “*Design of a Power Electronic Emulator for Renewable Energy Applications*” in Electric Machines and Drives Conference, IEMDC, Idaho, 2015.
2. H. Akbarian, P. Pillay, L. Lopes, “*Design of a Power Electronic Emulator for Series Hybrid Electric Vehicle Powertrains*” in VPPC, Montreal, 2015

## **1.7. SCOPE OF THE THESIS**

The main aspect of the thesis is to develop an emulator for emulation of the genset and HKECS output power to facilitate research for the purpose of an overall improvement of the system including a reduction in the fuel consumption rate per unit output power, decrease emission and increase efficiency of the genset.

Parallel operation of the genset and HKECS is discussed and verified in details and a new method is proposed to enforce the genset to work with less fuel consumption per unit output power, less pollution and more efficiency.

## **1.8. OUTLINE OF THE THESIS**

The thesis is organized in the following manner:

In chapter II, the mathematical models of the major units in a typical genset are provided and is shown how to use those models to control a VSI to emulate the genset. The droop control method is explained and related experimental implementations are carried out for verification.

Some important definitions including BSFC, emission and efficiency are provided to asses operation of a genset in chapter III and the relation of those parameters with respect to the output power are reviewed.

In chapter IV the HKECS principle is explained and is shown how to emulate the steady state available power of the HKECS using a CCVSI to be operated in parallel with the genset. It is also explained how to decouple the delivered  $P$  and the  $Q$  using dq-frame theory.

Parallel operation of multiple generator and its considerations are discussed in chapter V with a focus on the operation of the genset and HKECS emulators.

In chapter VI a novel method is presented to enforce the genset to operate in an ideal operating point using an alternative source of power and the method is applied on the parallel operation of the genset and the HKECS.

Finally conclusion of the thesis is presented in chapter VII.

Experimental validations are provided in each chapter.

### 2.1. INTRODUCTION

Diesel engine generator sets (also called gensets) are vastly used in remote areas and where the wired electricity is not available. A genset consists of two main units, ICE and generator (typically SG) coupled on the same shaft. Figure 2-1 shows a commercial diesel genset.



**Figure 2-1: A commercial genset**

A genset presents transient output voltage and frequency responses when its output power changes. To emulate the transient and steady state responses of a genset, transfer function of each components in a typical genset including electrical and mechanical parts are derived mathematically, and these models are used to produce the reference signals (with respect to the input mechanical power) for a VSI to generate the same behaviour as in a real genset.

Figure 2-2 illustrates schematic of the emulator. As is shown ICE is the prime mover which is coupled to a synchronous generator through the coupling shaft. Model of the generator is used to control the VSI to produce the reference signals for the PWM

generator and the resultant output voltage is filtered using LC LPF. Speed governor and AVR controllers are also included in the model to maintain the speed and voltage.

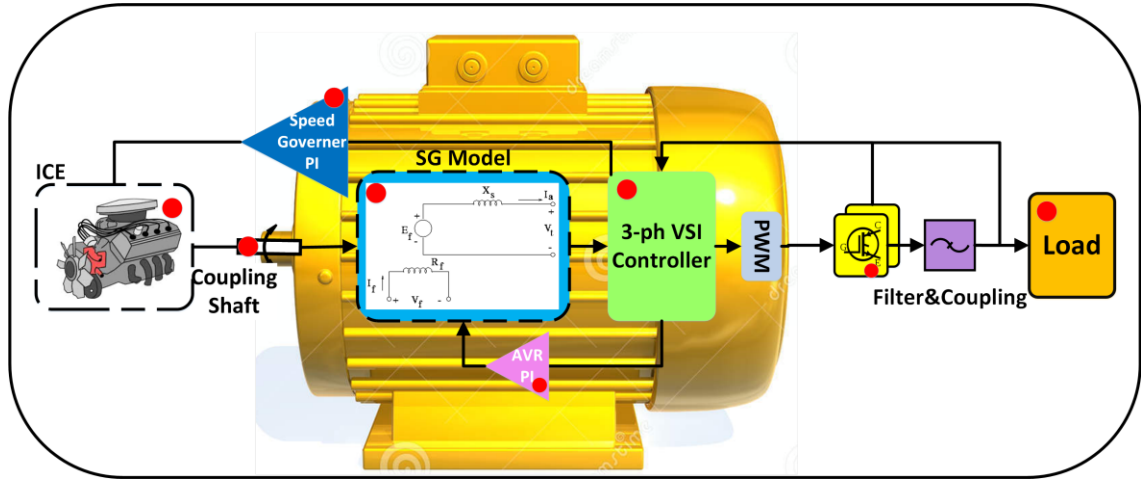


Figure 2-2: Connections and components in a commercial genset. Modelled components are marked with the red circle.

## 2.2. MODELING OF THE DIESEL ENGINE GENERATOR

A diesel engine generator block diagram in parallel with the HKECS in a microgrid is shown in Figure 2-3; consisting of five units: (1) Diesel engine; (2) Coupling shaft; (3) Electrical generator-typically synchronous generator (SG); (4) Speed governor; (5) Automatic voltage regulator (AVR).

In the following, each unit is modeled.

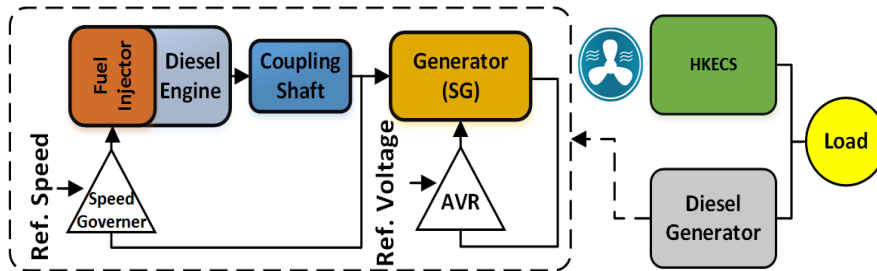


Figure 2-3: Diesel Engine Generator incorporated in a microgrid.

### 2.2.1. ICE Model

Modeling of the diesel engine (i.e. ICE) is well defined in the literature, which can be classified into three main parts: (1) Fuel injection gain (2) Fuel injection delay (3) Internal inertia. In this thesis for simplification, effect of the inertia is applied in the coupling shaft model. The resulting transfer function which simply includes the fuel injection dynamics and the time delay is [18-20]:

$$\frac{d\tau_{en}}{dt} = 1/t_e (-\tau_{en} + k_e u_\omega(t - t_d)) \quad (2.1)$$

$$h_e(s) = \frac{k_e e^{-t_d s}}{t_e s + 1} \quad (2.2)$$

where  $k_e$  is engine gain,  $t_d$  is fuel injection delay time,  $t_e$  is fuel injection (engine) time constant,  $u_\omega$  is governor reference speed (RPM),  $\tau_{en}$  is engine produced torque and  $h_e(s)$  is transfer function of engine in the s domain.

### 2.2.2. Flexible Coupling Shaft Model

Based on the Newton's second law for a rotational mass, dynamics of the flexible shaft and associated inertia can be described as [20]:

$$J_{en} \frac{d\omega_{en}}{dt} = \tau_{en} - \tau_r - \tau_s - \tau_D \quad (2.3)$$

$$J_{ge} \frac{d\omega_{ge}}{dt} = \tau_s + \tau_D - \tau_{ge} \quad (2.4)$$

where  $J_{en}$  and  $J_{ge}$  are diesel engine and generator inertia,  $\omega_{en}$  and  $\omega_{ge}$  are engine and generator angular speeds,  $\tau_{en}$  and  $\tau_r$  are engine and reciprocating inertia torques,  $\tau_s$  and  $\tau_D$  are the torsional stiffness and damping torque, and  $\tau_{ge}$  is the transmitted torque to the generator. Figure 2-4 shows the mechanical equivalent for (2.3) and (2.4).

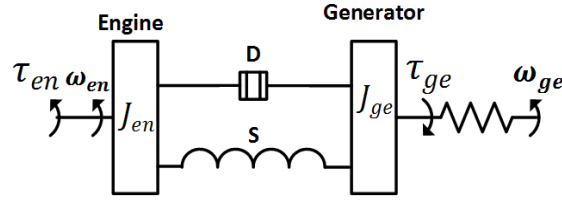


Figure 2-4: Diesel engine and generator mechanical models.

### 2.2.3. Synchronous Generator Model

The resulting output torque of the shaft produces the rotational speed on the generator shaft which then converts the mechanical torque to the related output electrical torque. In order to investigate the output electrical torque (i.e. electrical power), the exact model of the generator (typically SG) should be known. Among many works which have been done to model the SG, dq-modeling most precisely describes the transient behavior of the machine in comparison to conventional models. In this thesis, SG is represented by the dq-frame model 2.1 of IEEE Std. 1110-2002 [21]. Output of the SG, which is a voltage signal in the dq-frame, will then be considered as the reference voltage signals for the VSI to produce the output emulated voltage.

The well-known equations describing the SG model in the dq-frame are [22]:

$$v_d = -R_s i_d - \omega_r \lambda_q + p \lambda_d \quad (2.5)$$

$$v_q = -R_s i_q + \omega_r \lambda_d + p \lambda_q \quad (2.6)$$

$$v_{fd} = R_{fd} i_{fd} + p \lambda_{fd} \quad (2.7)$$

$$v_{kd} = R_{kd} i_{kd} + p \lambda_{kd} \quad (2.8)$$

$$v_{kq} = R_{kq} i_{kq} + p \lambda_{kq} \quad (2.9)$$

$$\lambda_d = -L_l i_d + L_{md} (i_{fd} + i_{kd} - i_d) \quad (2.10)$$

$$\lambda_q = -L_l i_q + L_{mq} (i_{kq} - i_q) \quad (2.11)$$

$$\lambda_{fd} = L_{lfd}i_{fd} + L_{md}(i_{fd}+i_{kd} - i_d) \quad (2.12)$$

$$\lambda_{kd} = L_{lkd}i_{kd} + L_{md}(i_{fd}+i_{kd} - i_d) \quad (2.13)$$

$$\lambda_{kq} = L_{lkq}i_{kq} + L_{mq}(i_{kq} - i_q) \quad (2.14)$$

where,  $p$  is the derivative function ( $d/dt$ ).

The electrical and mechanical torque are also related in the following equation:

$$T_e = -J \left( \frac{2}{P} \right) p\omega_r + T_m \quad (2.15)$$

where  $J$  is the total inertia (rotor and the load connected to the rotor) and  $P$  is the number of poles. To solve this equation,  $T_e$  can also be found as:

$$T_e = \frac{3}{2} \left( \frac{P}{2} \right) (\lambda_d i_q - \lambda_q i_d) \quad (2.16)$$

Figure. 2-5 shows the equivalent circuit for the above equations.

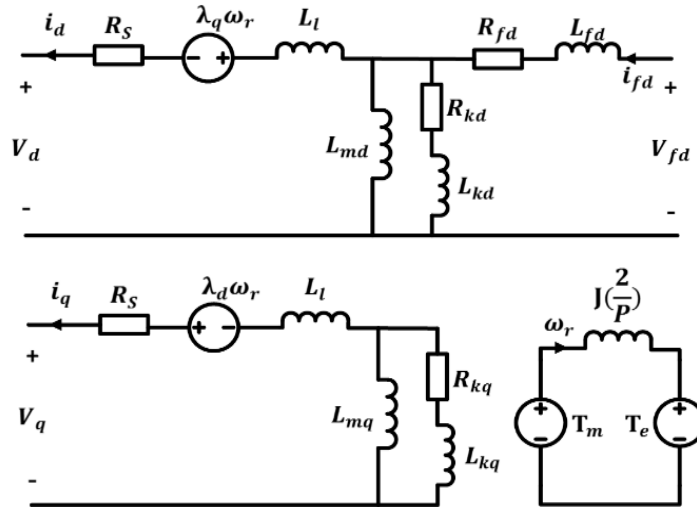


Figure. 2-5: SG equivalent model in dq-frame.

For implementation, the input parameters to the SG model are the actual measured output currents of the inverter in the dq-frame ( $i_d, i_q$ ) which reflect the load and the desired rotational shaft speed which is determined by the speed governor (and droop controller); in addition to the value of the field winding voltage which is determined by the AVR. The output parameter of the SG model is the voltage reference signal for the VSI.

#### 2.2.4. Speed Governor

The speed governor is essentially a closed loop (typically PI) controller to drive the actual speed to its reference value after the load changes. Since the frequency finally converges to a fixed value, hence also called isochronous operation.

For the PI controller, the output speed signal to the engine which is the fuel injection reference signal can be expressed as:

$$y_{\omega en} = \left(k_p + \frac{k_i}{s}\right)(\omega_{enref} - \omega_{enact}) \quad (2.17)$$

Figure. 2-6 shows the block diagram representation of the speed governor.

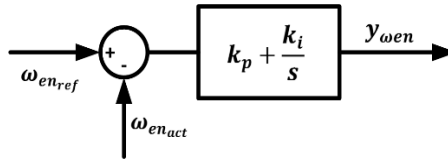


Figure. 2-6: PI controller for speed governor.

It is shown in “section 2.4” how to control  $\omega_{enref}$  to implement a droop controller.

#### 2.2.5. Automatic Voltage Regulator

Aim of using the AVR is to maintain terminal voltage of the SG regulated while load changes. Similar to speed governor, a PI controller can be configured to control terminal voltage of the SG. Since field voltage of the SG is assumed to be supplied with a thyristor

controlled rectified voltage, the rectifier dynamics should be also included in the control loop. The rectifier can be simplified as a first order filter with linear gain ( $k_{rec}$ ) and a time delay ( $t_{del}$ ).

IEEE Std. 421.5 is used for the AVR modeling. The corresponding equations can be obtained from [9]. The resulting block diagram is shown in Figure. 2-7.

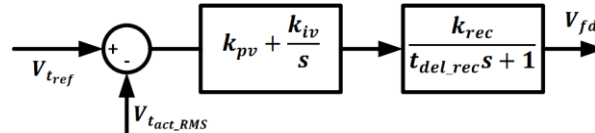


Figure. 2-7: Automatic voltage regulator for the diesel engine generator.

### 2.3. CURRENT AND VOLTAGE CONTROLLED VSI

Voltage source inverters are widely used in power generation and grid connected applications [8, 23]. Since the output voltage characteristic of the inverter is of interest, a VSI with only a voltage control loop can be designed to emulate the output voltage, but including an inner current controller speeds up the convergence to the reference value and makes a much tighter controlled output voltage signal. Figure. 2-8 shows a block diagram of a voltage source inverter with a main voltage controller and an inner current control loop. The main parts of the inverter consist of: three-phase full bridge, LC low pass filter and the load.

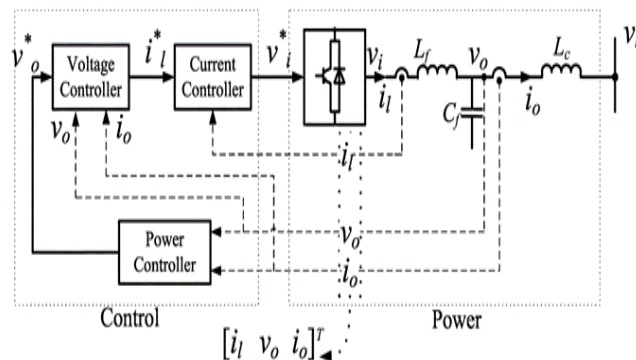


Figure. 2-8: VSI block diagram [24].

As mentioned before, reference signals (i.e. amplitude, phase and frequency) for the VSI are determined by the SG model in the dq-frame as in [25]. Having the input reference voltage and frequency of the inverter, voltage and current control loops in the VSI produce the required duty cycle of the PWM for 3-phase full-bridge switches so that the output voltage emulates behaviour of a diesel engine generator. To emulate the output voltage characteristic of a diesel engine generator, the SG output voltages and currents are monitored and fed as the reference signals of the VSI. For the outer voltage controller loop, inputs to the controller are referenced voltages ( $v^*_d, v^*_q$ ) and the output are the dq-frame currents ( $i^*_d, i^*_q$ ) which act as the reference for the current controller loop. The current control loop on the other hand, determine the modulation voltage for the PWM to generate the output voltage.

The dq-frame KVL and KCL equations of the inverter for the basic circuit of a VSI shown in Figure. 2-8 are:

$$L_f \frac{di_{fd}}{dt} = v_{id} - r_f i_{fd} - v_{od} + L_f \omega i_{fq} \quad (2.18)$$

$$L_f \frac{di_{fq}}{dt} = v_{iq} - r_f i_{fq} - v_{oq} - L_f \omega i_{fd} \quad (2.19)$$

$$C_f \frac{dv_{od}}{dt} = i_{fd} - i_{od} + \omega C_f v_{oq} \quad (2.20)$$

$$C_f \frac{dv_{oq}}{dt} = i_{fq} - i_{oq} - \omega C_f v_{od} \quad (2.21)$$

Based on (2.18-2.21), control diagram of the inverter is derived as is shown in Figure. 2-9 which is discussed in [24].

For a 5 kVA commercial genset a VSI with the same rated power is designed. Related parameters are shown in Table II in the appendix.

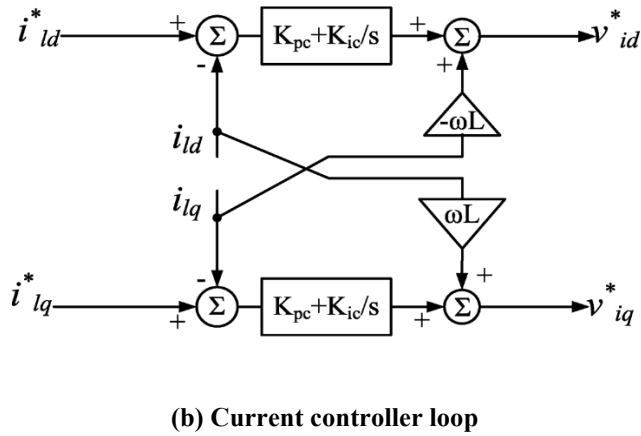
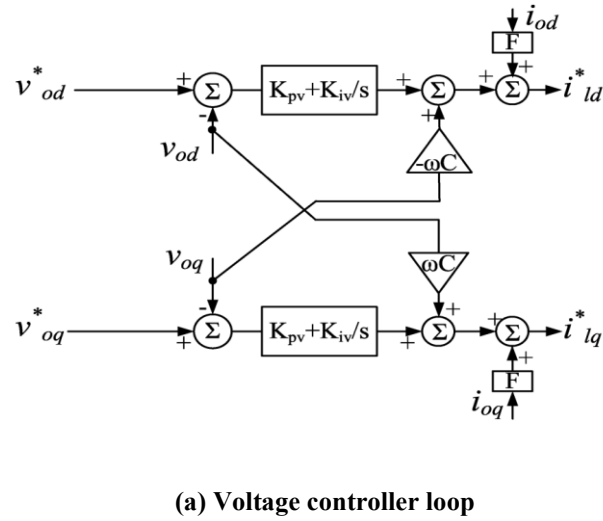


Figure. 2-9: (a) Voltage and (b) current controller loops block diagrams [24].

## 2.4. DROOP CONTROLLER

For parallel operation of generators, a droop controller should be included for proper sharing of the load between generators. For a stable load sharing, the frequency of each unit (i.e. governor reference speed) has to drop while the load (i.e. output power) increases.

The droop factor percentage can be defined as [26]:

$$D = \frac{\Delta_f}{\Delta_P} = \frac{\omega_{NL} - \omega_{FL}}{\omega_0} \quad (2.22)$$

where  $\omega_{NL}$  is the no load speed,  $\omega_{FL}$  is the full load speed, and  $\omega_0$  is the rated speed.

Consequently the following block diagram determines the reference speed for the governor based on droop percentage and the power.

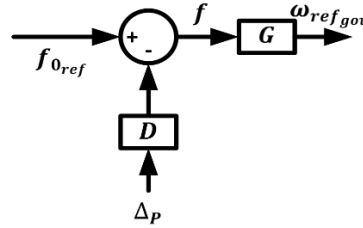


**Figure. 2-10: Speed-Droop governor.**

where  $G = \frac{4\pi}{P}$  and  $P$  is number of poles in the SG.

## 2.5. EXPERIMENTAL IMPLEMENTATION AND VALIDATION

For experimental validation, a test bench including one 3-phase IGBT switch pack, filters and controller is built to emulate the genset as is shown in Figure. 2-11. The designed inverter is rated at 5 kVA, 110 V – 60 Hz for continuous operation. The control algorithm is first simulated in Simulink and then implemented in dSpace where the output of the SG model and a simple  $P$ - $F$  droop controller generate the reference voltage and frequency for the inverter. The controller design procedure is provided in appendix and the derived parameters for the controllers are listed in TABLE I through TABLE VII. Input to the SG is the rotor shaft torque and speed which are determined by the diesel generator model. The controller is developed in dSpace, with the DS-1103 controller for capturing and controlling the digital and analog signals. Since measured signals are contaminated with noise, active filters are designed for noise reduction and phase shift (due to the voltage and current sensors phase shift) compensation using AD analog filter design tools.

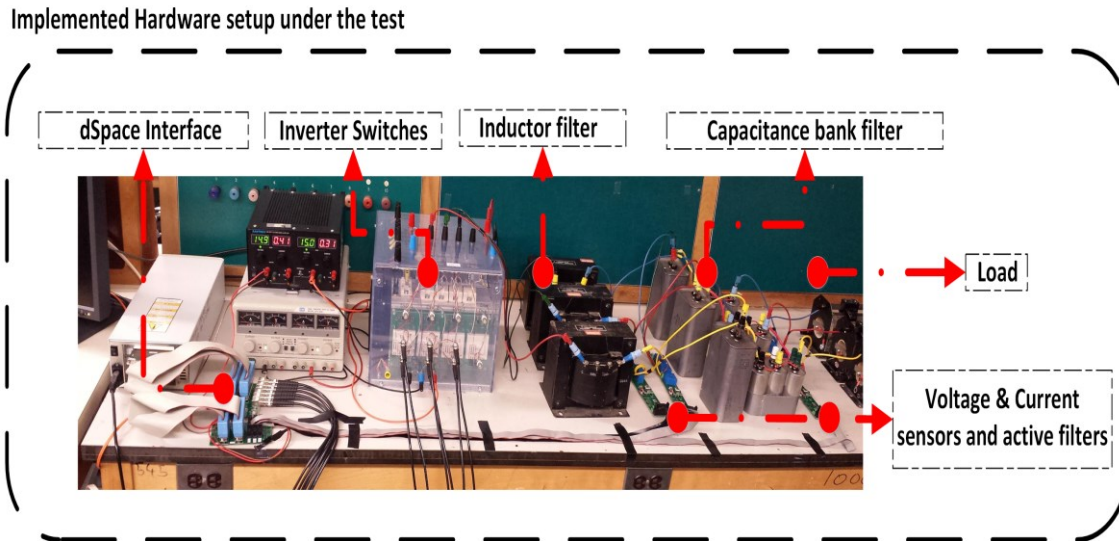


Figure. 2-11: Implemented hardware setup of the Emulator under the test.

### 2.5.1. Individual Diesel Genset Experimental Test

Tests are conducted in two different modes; isochronous (Fixed frequency) and droop-controlled mode.

#### a. Isochronous mode of operation

In this mode, the reference frequency of the genset is constant. The voltage and frequency vary dynamically according to the disturbance hence the output voltage amplitude and frequency behavior of the VSI is of interest while the emulator experiences a step load variation. Figure. 2-12 illustrates the output  $V_a$  versus  $V_b$  phase voltages to verify quality of the sinusoidal voltage. The non-distorted ellipse with the  $120^\circ$  initial angle in Figure. 2-12 (b) generally shows the quality of the output voltage. With a 6 kHz SPWM modulation a THD is measured to be 0.89 % for a  $20\Omega$  load.

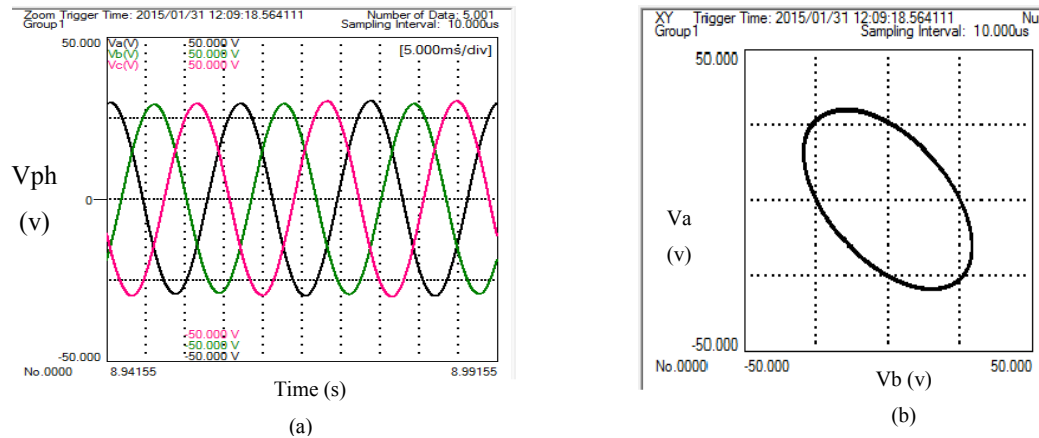


**Figure. 2-12: (a) Measured output voltage in the abc frame (Scale=4.7:1); (b) X-Y graph to verify the quality of output voltage (Scale=4.7:1).**

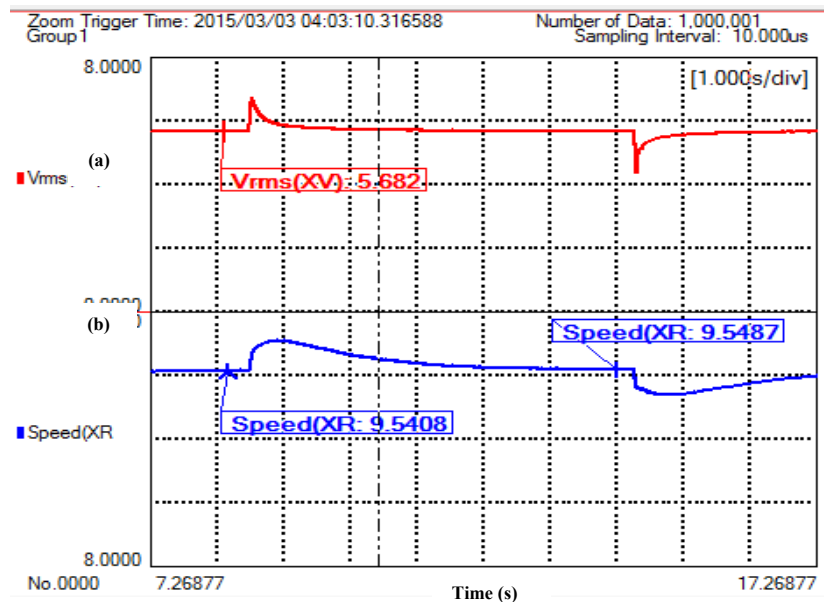


**Figure. 2-13: Measured output signal of the Emulator in response to a step load change (a) Measured output RMS voltage (Scale=20:1) (b) Actual shaft RPM of the SG (Scale=600/π:1).**

Figure. 2-13 shows the RMS amplitude and frequency of the output measured voltage of the implemented emulator for a sample step load changing from 900 W to 3.5 kW.

At  $t=8.7$  sec, load decreases from 3.5 kW to 900 W. It is shown (due to the inertia) how the SG shaft speed change while load changes. At  $t=14.3$  sec, load varies from 900 W to

3.5 kW. As is shown since the genset is working in isochronous mode, the settling value of frequency before and after the turbulence is the same value, independent of the output power.

To validate the results, they are compared with other publications results. Because of the various system and controllers types, no two different configurations of gensets behave exactly in the same way, however the general behavior of the genset could be compared.

The same typical behavior is studied in [18]. It is shown in Figure. 2-14 how the speed of the generator changes in response to a step increase in the load.

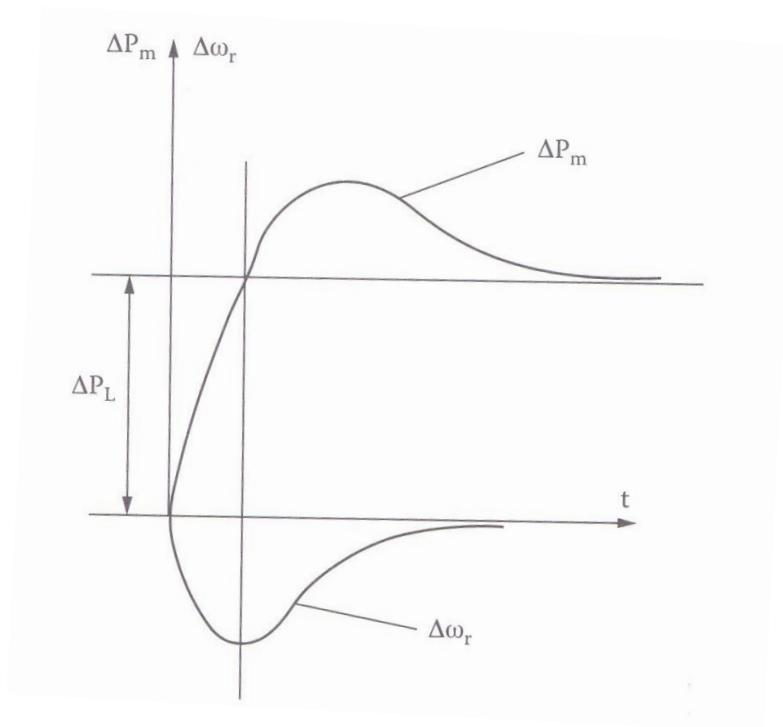


**Figure. 2-14: Response to a step load increase in isochronous speed governor [18].**

The same behavior is also discussed in [15]. As is shown in Figure. 2-15, for the 0% droop (Isochronous mode) when the load is increased by 50% at the time  $t=0.2$  sec, the frequency has dropped and then the speed governor controller has tried to bring the frequency back to its original value.

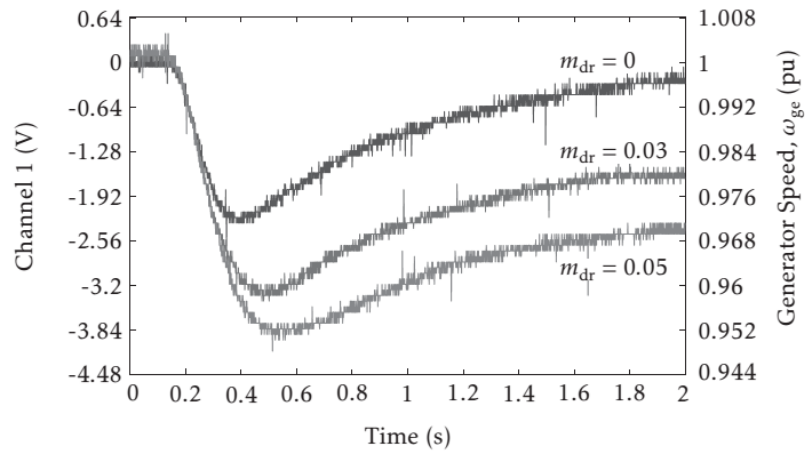


**Figure. 2-15: Transient response of the emulator for different values of droop studied in [15].**

For the voltage amplitude, no major publication is found to validate the voltage amplitude behavior, however the behavior shown in Figure. 2-13 (a), is expected when the equivalent circuit shown in Figure. 2-5 is studied. When the load increases the output voltage drops temporarily and then the AVR brings the voltage back to its reference value.

### **b. Droop controlled mode of operation**

Based on the method which was discussed in “section 2.4”, for a 1%, 3% and 5% droop, Figure. 2-16 and Figure. 2-19 show the output frequency and voltage amplitude of the emulator. (The maximum power for the droop slope calculations is set to 5kW,  $f_0$  is 60 Hz and the no load frequency ( $f_{NL}$ ) is 62 Hz, which means at 5kW output power, the output frequency will experience 5% decrease for 5% droop (i.e. 3Hz) etc.). It is shown how the output frequency changes in response to a step change in the output power from 1 kW to 3.5 kW while voltage amplitude does not change.

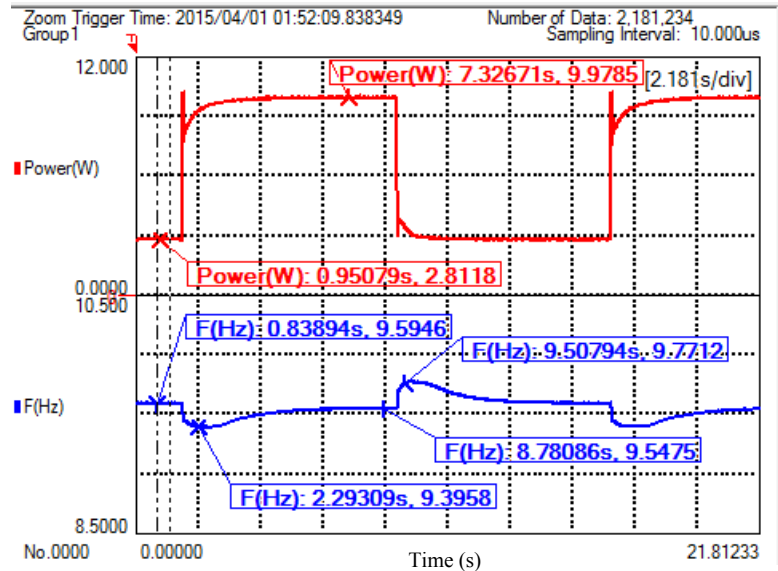


Figure. 2-16. Output frequency change during a step load change from 1 kW to 3.5 kW for 1% droop. (Power scale: 350:1, Frequency scale:  $81/4\pi:1$ ).

The Figure. 2-16 and Figure. 2-19 show how the transient behavior of the genset frequency is when the load changes. As is shown when the load increases the frequency experiences a transient change and settles to a fixed value. As is shown, frequency drops to 61.9 Hz for output power of 1kW as is expected to be:

$$f = f_{NL} - f_0 \times D \times \frac{P_{out}}{5kW} = 62 - 0.6 \times \frac{1kW}{5kW} = 61.88 \quad (2.23)$$

The droop line for a 1% droop is shown:

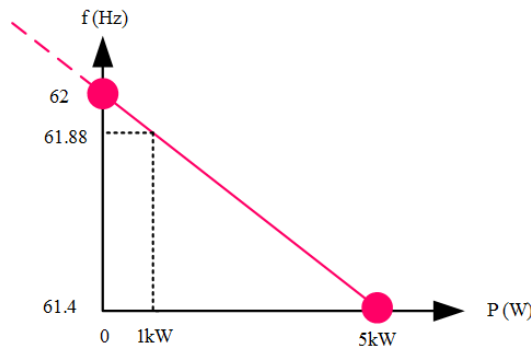
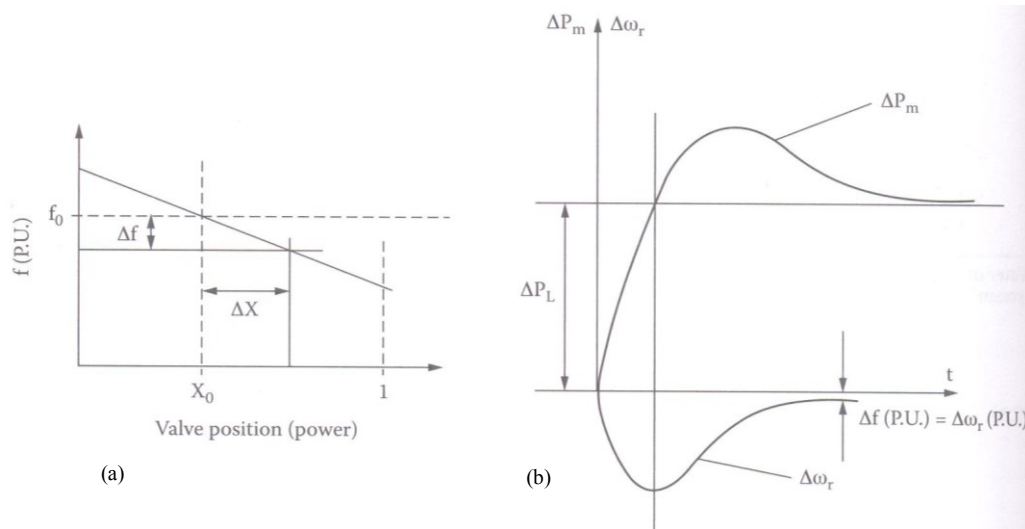


Figure. 2-17. The droop line for a 1% droop.

For the result validation with the other publications, the speed (frequency) behavior studied in [18] is shown in Figure. 2-18. As is shown the typical behavior induces a transient drop in the speed when the load increases. The settling speed depend on the value of the delivered power.

The same behavior is shown in Figure. 2-15 for different droop percentages.



**Figure. 2-18. The response to a step load increase in a droop controlled speed governor studied in [18]. (a) Frequency power droop (b) Response to step load power.**

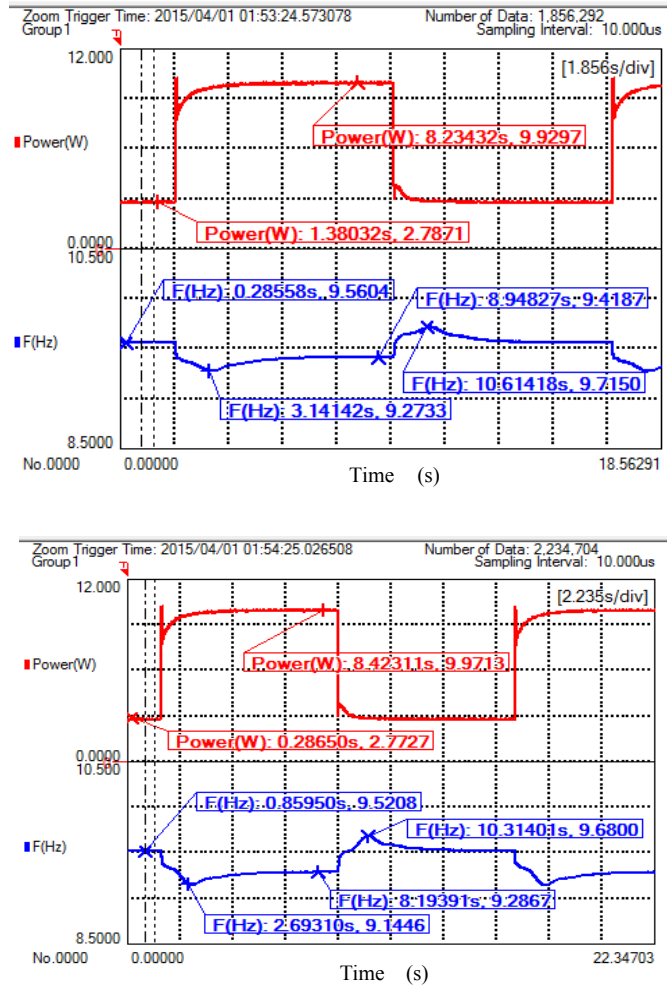


Figure. 2-19. Output frequency change during a load step change from 1 kW to 3.5 kW for (a) 3% and (b) 5% droop. (Power scale: 350:1, Frequency scale:  $81/4\pi$ :1).

## 2.6. SUMMARY

A VSI is designed and controlled to emulate a genset. Mathematical models of the different units in a genset are used to produce the reference signals for a VSI. Hence the output signals of the VSI emulates behavior of a real genset. The VSI is designed with the voltage and current controllers in the dq-frame.

Controller blocks which are typically used in commercial gensets including AVR, speed governor and droop controllers are designed and included in the VSI controller algorithm.

The emulator algorithm is implemented in the Simulink and dspace workspaces and additional voltage and current active filters are designed and built for noise reduction purposes in the controller. The filter time delay constants and transfer functions are considered in the VSI controller.

## **2.7. CONCLUSIONS**

The measured output waveforms of the emulator are observed to be compatible with the other publications results and show satisfactory results in terms of the quality and similarity of the generated output voltage with real commercial gensets studied in the those publications. The transient and steady state responses of the controllers are considered to be within an acceptable range.

## **2.8. CONTRIBUTIONS**

1. A voltage and current controlled VSI in dq-frame is designed. The input reference signals are fed by mathematically modeled parts of a typical genset.
2. Additional auxiliary controllers including AVR, speed governor and droop controllers are designed to control the desired parameters of the genset as is in a real genset.
3. Some additional required equipment including voltage and current measurement devices and active filters are designed and built for the feedback measurement of the VSI controllers.

---

## Chapter 3. BSFC, EMISSION AND EFFICIENCY VERSUS POWER IN AN ICE

---

### 3.1. INTRODUCTION

Internal combustion engines (ICE) are energy conversion devices that extract stored energy in a fuel through the combustion process and deliver mechanical power. The devices are also known as heat engines in a broader sense. Compromise is often necessary to deliver acceptable efficiency, and performance through its performance regime. The ICE could be employed in an operating range to enhance the fuel economy and reduce emission. Fuel economy depends on the operating point of the ICE, while emission control units target eliminating harmful pollutants from the exhaust stream [10].

There exists an optimal operating point for a genset to operate in, to have the best environment impact. It will be shown how the output power delivered by the ICE affects the operating point of the ICE in terms of efficiency, emission and fuel consumption. Later in the next chapter will be shown how to control other parallel sources of energy in a company with the genset to enforce the genset to operate in the ideal mode in terms of fuel consumption efficiency.

In the following, some practical terms used to verify performance of an ICE are defined.

### 3.2. BSFC

In engine test, fuel consumption is measured as a flow rate-(mass flow) per unit time,  $\dot{m}_f$  ( $\frac{gr}{sec}$ ). A more useful term is the specific fuel consumption (SFC) - the fuel flow rate per useful output power. It measures how efficiently an engine is using the fuel supply to produce work.

$$sfc = \frac{\dot{m}_f}{P} \quad (3.1)$$

where  $\dot{m}_f$  is the fuel flow rate and  $P$  is the engine power. If the engine power is measured as the net power from the crankshaft, the specific fuel consumption is called brake specific fuel consumption (BSFC). The SFC and BSFC are usually measured in SI units by the gram numbers of fuel consumed per kW power output per hour ( $g/kWh$ ). Obviously low values of SFC or BSFC are desirable. Typical best values of BSFC is around 250 to 270  $g/kWh$  [27].

This ratio (BSFC) is not constant and varies with respect to the output power. Except for low (under 25%) and high (more than 75%) power levels (where is estimated as a linear function as is shown in Figure. 3-1), this function is often well approximated by a positive quadratic function of the type [28]:

$$BSFC(P) = k(P - P_{opt})^2 + BSFC_{min} \quad (3.2)$$

where  $P$  is the output power of the ICE, and  $P_{opt}$  is the power in which the minimum BSFC can be achieved ( $BSFC_{min}$ ).

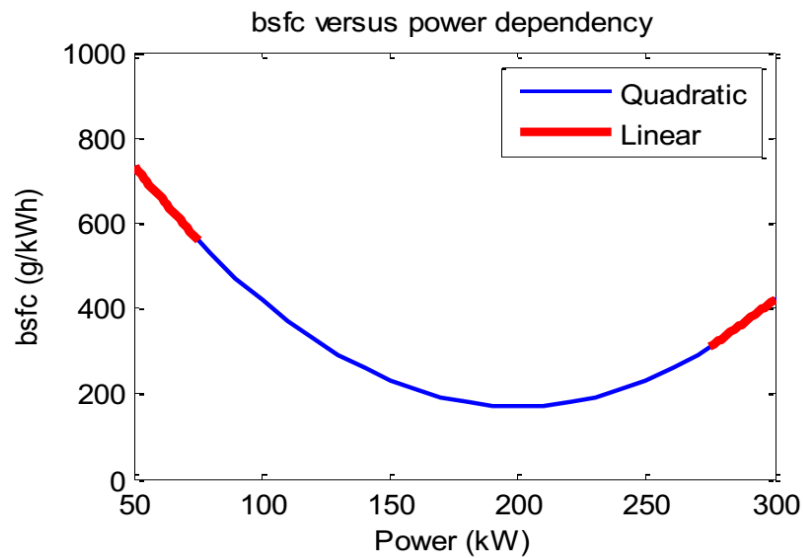


**Figure. 3-1. Quadratic and linear approximations for BSFC versus Power dependency for a sample ICE [28].**

For linear operating ranges that correspond to a very high and a very low power level, a linear approximation of the form:

$$BSFC(P) = BSFC_{max} + cP \quad (3.3)$$

Is introduced where  $c$  is a negative constant for small  $P$  and is positive for large  $P$  [28].

### 3.3. FUEL EFFICIENCY VERSUS POWER

Normally, a dimensionless parameter that relates the desirable engine output power to the necessary input fuel flow would have more fundamental value. The ratio of the work produced per cycle to the amount of fuel energy supplied per cycle that can be released in the combustion process is commonly used for this purpose. It is a measure of the engine efficiency (fuel conversion efficiency) as is shown below:

$$\eta_f = \frac{W_c}{m_f Q_{HV}} = \frac{P}{\dot{m}_f Q_{HV}} \quad (3.5)$$

where  $W_c$  is work done in one cycle,  $m_f$  is the fuel mass consumed per cycle, and  $Q_{HV}$  is heating value of the fuel.

Fuel efficiency can be expressed by SFC as:

$$\eta_f = \frac{1}{sfc Q_{HV}} \quad (3.6)$$

### 3.4. ICE EFFICIENCY VERSUS POWER

To predict the ICE efficiency in terms of the output power, and for the purpose of setting the ideal operating point, the efficiency behaviour of the ICE can be investigated with respect to the speed and output torque of the engine as is shown in Figure. 3-2.

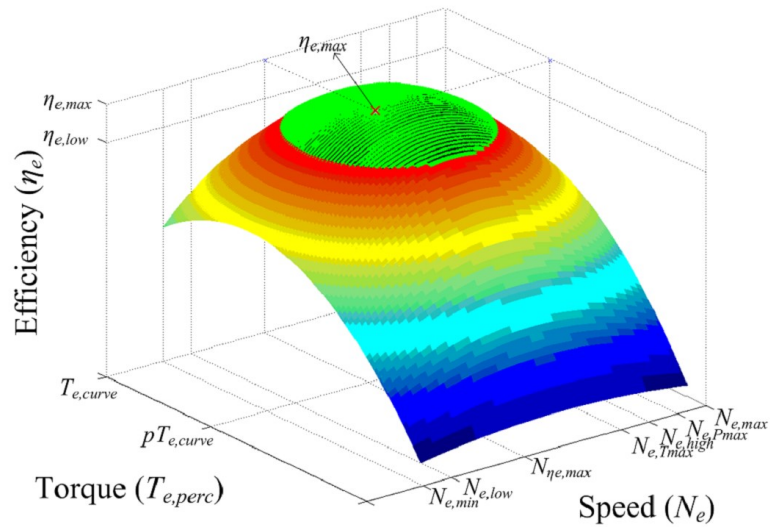


Figure. 3-2. Example ICE efficiency model. The high efficient region is highlighted by the shaded green cap of the 3D model [29].

Efficiency map of the different ICEs varies by type and output power capacity but they all have typically the same behaviour as shown in Figure. 3-2. Since the ICE in a genset operates at almost a fixed speed, the output power and thus efficiency could be defined as an intersection of a plane and surface in Figure. 3-2 which yields a quadratic function curve. Efficiency versus power can be directly shown as in Figure. 3-3[1].

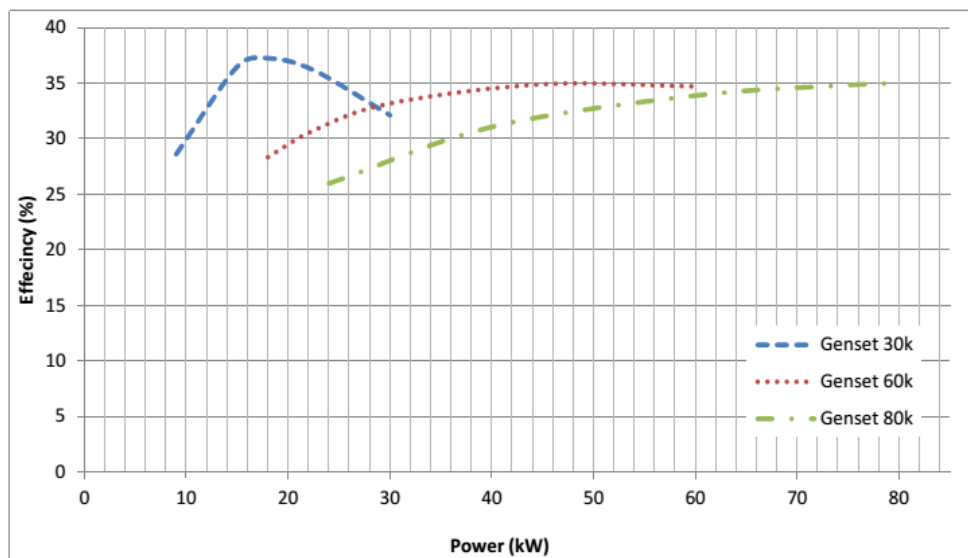


Figure. 3-3. Efficiency versus power in three different gensets studied in [1].

### 3.5. EMISSION VERSUS POWER

Levels of the emissions of oxides of nitrogen, carbon monoxide, unburned hydro carbons, and particles are important engine operating pollutant characteristics. The concentrations of gaseous emissions in the engine exhausts are usually measured in parts per million or percent by volume (mole fraction). Specific emissions are defined as the flow of the pollutant per output power:

$$sNO_x = \frac{\dot{m}_{NO_x}}{P} \quad (3.7)$$

$$sCO = \frac{\dot{m}_{CO}}{P} \quad (3.8)$$

$$sHC = \frac{\dot{m}_{HC}}{P} \quad (3.9)$$

$$sPart = \frac{\dot{m}_{part}}{P} \quad (3.10)$$

Emissions of the ICEs are a function of the output power of the engine. Emissions typically increase with an increase in the output power as is shown in Figure. 3-4.

One can set the operating point of the genset to operate with the least pollute.

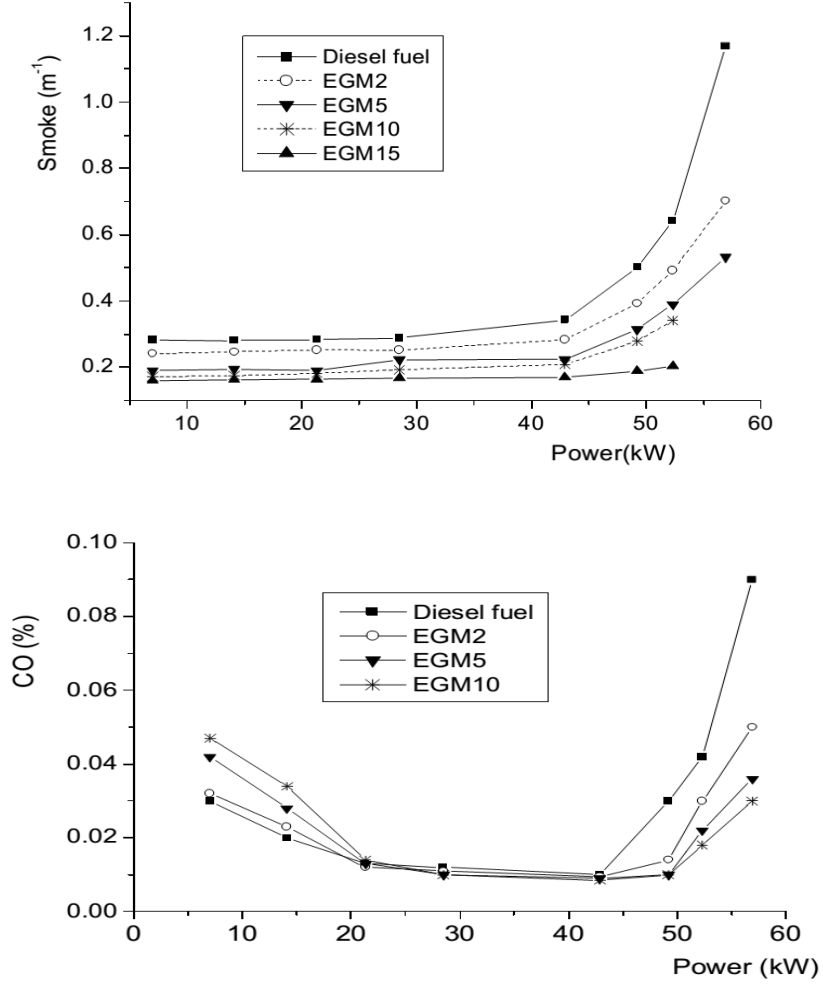


Figure. 3-4. Sample emission characteristic which is studied in [30].

### 3.6. FUEL CONSUMPTION COST DURING THE OPERATION

Except for the transient operation, total fuel consumption cost during the operation of the ICE in a genset can be approximated as:

$$C = \int_0^{P_{max}} C_f \times BSFC(P) \times p(P) \times T_{total} \times dP \quad (3.4)$$

where  $C_f$ , is cost of the fuel per gram,  $p(P)$  is probability of the engine producing power at level  $P$  and  $T_{total}$  is the total run time.

### **3.7. SUMMARY**

Some useful terms for the operation assessment of the ICEs defined in the literature are reviewed. These parameters are to be used in the following chapters to control other parallel sources of energy in a company with the genset to enforce the genset to operate in the ideal operation in terms of fuel consumption, emission and efficiency.

#### 4.1. INTRODUCTION

HKECS refers to conversion of the flowing fluid (e.g. water) energy into electricity.

Hydrokinetics energy has a tremendous potential to be considered as one of the alternative sources to the conventional fuel based electricity generators.

The US wave and current energy resource potential that could be credibly harnessed (the potential amount is about 2100 *TWh/yr*), is currently about 400 *TWh/yr* or about 10% of national energy demand. Assuming an extraction of 15% wave to mechanical energy (which is limited by device spacing, device absorption and sea space constraints), typical power train efficiencies of 90% and a plant availability of 90%, the electricity produced is about 260 *TWh/yr* or equal to an average power of 30,000 MW (rated capacity of about 90,000 MW). This amount is approximately equal to the total 2004 energy generation from conventional hydro power (which is about 6.5% of total US electricity supply). The Canadian wave energy resource was studied by Natural Resources Canada (NRC) and found to be about 1,600 *TWh/yr* [31]. (Figure. 4-1).

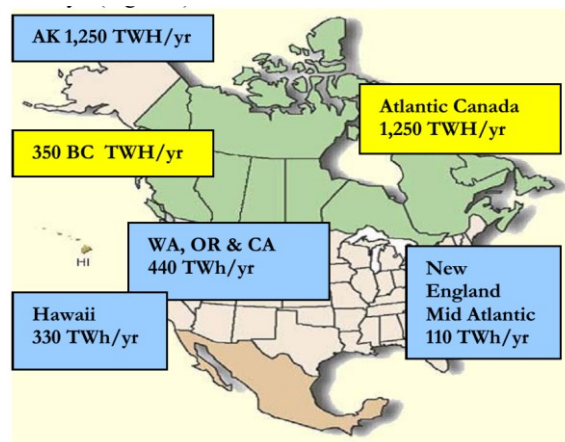


Figure. 4-1. Wave energy resource estimation [31].

There are various methods to harvest the fluid water energy; most of known are ocean current, waves, and river in-stream currents.

The energy conversion devices needed to convert the kinetic energy in rivers are very similar to those for tidal; the major differences being that river current streams are unidirectional and composed of fresh water [31].

Hydrokinetic energy harvesting is fundamentally similar to the wind.

Hydrokinetic devices typically use vertical or horizontal axis turbines similar to those developed for wind generation; however, because water is approximately 850 times denser than air, the amount of energy generated by a hydrokinetic device is much greater than that produced by a wind turbine of equal diameter. In addition, river and tidal flow do not fluctuate as dramatically from moment to moment as wind does. This predictability benefit is particularly true for tidal energy. It can be predicted years in advance and is not affected by precipitation or evapo-transpiration [32].

#### 4.2. PREDICTING THE AVAILABLE POWER AND TORQUE

For a water channel flow, available power in the cross section of a turbine is given by:

$$P_{turb} = \frac{1}{2} C_p(\lambda) \rho_w A_r V_w^3 \quad (4.1)$$

where  $C_p(\lambda)$  is the turbine power coefficient,  $\rho_w$  is the water density,  $A_r$  is the rotor cross section area and  $V_w$  is the water velocity.

Thus if the turbine is coupled directly to the generator, the produced torque on the generators shaft is given by:

$$\tau_{shaft} = \frac{P_{turb}}{\omega_{shaft}} = \frac{C_p(\lambda) \rho_w A_r V_w^3}{2\omega_{shaft}} \quad (4.2)$$

The dynamic response of the flowing water would depend on the torque transferred to the shaft. Only the steady state response of the output power is studied.

Since the dynamic response of the system is typically faster than the actual power flow and because the output stage of the system is driven by an inverter which regulates the output frequency and voltage amplitude connected to the grid, the entire system has been modelled as a power generation unit with an output  $PQ$  characteristic based on the available water flow power. Some power loss in each unit is also defined, hence the output power would be proportional to the available input power. Since the mechanical inertia and time delay constants are not defined in the model, the model is valid only for the steady state and with the assumption of the availability of the required power.

#### 4.3. CONFIGURATION OF A HKECS

Since the available hydrokinetic power varies with time, the output voltage of the generator must be regulated to be useful. Shown in Figure. 4-2., HKECSs consist of three main units: 1- Energy harvest and generator, 2- Rectifier, 3- Inverter.

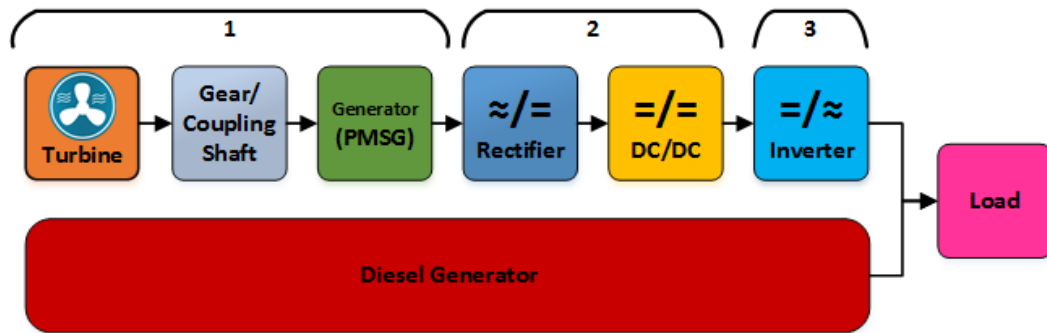


Figure. 4-2. A typical structure of the HKECS in parallel with a genset.

#### 4.4. POWER DELIVERY TO THE LOAD

A HKECS operated in parallel with a Genset to supply a load, could be considered as a grid tied inverter; as is shown in Figure. 4-2. For a grid tied inverter shown in Figure. 4-3, flow of the  $P$  and  $Q$  are given by:

$$P = 3 \frac{EV}{X} \sin(\theta_E - \theta_V) \quad (4.3)$$

$$Q = 3 \frac{E}{X} (E - V \cos(\Theta_E - \Theta_V)) \quad (4.4)$$

where  $E$  is the VSI terminal voltage,  $V$  is the grid bus voltage,  $\Theta_E$  and  $\Theta_V$  are VSI and grid bus voltage phases respectively.

As is shown, magnitude of active ( $P$ ) and reactive ( $Q$ ) powers delivered by an inverter to the grid are coupled together and it is cumbersome to control them separately using voltage amplitude and phase of the two sources.

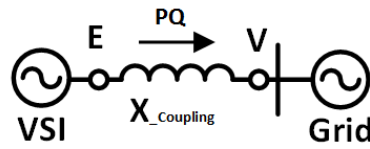


Figure. 4-3. A grid tied VSI.

It will be shown how to decouple and control active and reactive powers through controlling the dq components of the output current using dq-frame theory. Since the decoupled current components are of interest, a CCVSI should be used. The  $i_d$  and  $i_q$  components of a CCVSI is controlled in dq-frame to deliver the required active power according to HK power profile.

#### 4.4.1. Decoupled Control of the $PQ$

Active power ( $P$ ) and reactive power ( $Q$ ) can be represented in dq-frame as:

$$P = v_d i_d + v_q i_q \quad (4.5)$$

$$Q = v_d i_q - v_q i_d \quad (4.6)$$

If the VSI shown in Figure. 4-3 being applied the feedback voltage from point  $V$  of the grid instead of the point  $E$ , then the,  $v_d$  and  $v_d$  are some known values determined by the

grid; consequently the system of equations in (4.5) and (4.6) can be solved for a unique  $i_d$  and  $i_q$ .

With a proposed diagram shown in Figure. 4-4, for any arbitrary values of  $PQ$ ,  $i_d$  and  $i_q$  would be set for decoupled control of  $PQ$ .

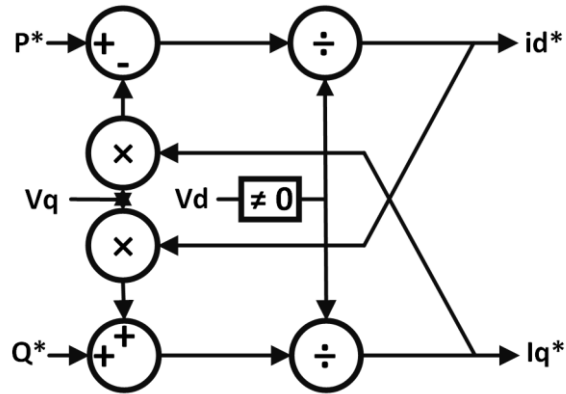


Figure. 4-4. Power controller of the VSI;  $i_d$  and  $i_q$  to decouple  $PQ$ .

#### 4.4.2. Current Controlled VSI

The HKECS is placed close to the genset thus the bus voltage is close to the genset output voltage and since the output voltage would be determined by the grid (genset), no voltage controller for the HKECS is required, thus the same controller topology discussed in “section II. B” is used without voltage controller loop. Output of the power controller shown in Figure. 2-8 feeds the current controller shown in Figure. 2-9 (b). Related controller coefficients are shown in TABLE III.

Genset determines output voltage amplitude and phase of the CCVSI and CCVSI injects or absorbs some power through the current while the amplitude of the voltage is dictated by the genset. The dq components of the grid voltage are added as a feedforward voltage for strict tracking of the grid voltage and to decrease the convergence time of the CCVSI controller to adjust its output voltage. This also enforces the inverter to track the grid voltage at the start up and avoids the start-up inrush current.

Figure. 4-5 shows the resulting CCVSI topology.

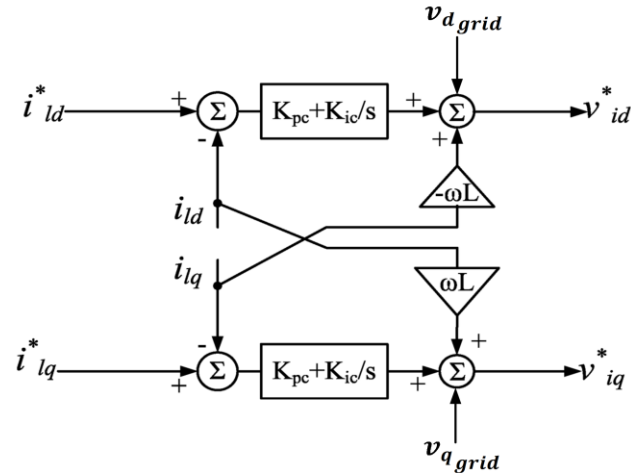


Figure. 4-5. CCVSI topology.

#### 4.5. EXPERIMENTAL IMPLEMENTATION AND VALIDATION

During the experimental tests, the HKECS emulator is operated in parallel with the diesel engine generator emulator in a configuration of shown in Figure. 4-2 which was discussed in “4.4.1”Chapter 2. to show how the  $P$  and  $Q$  are controlled separately.

##### 4.5.1. Coupled $PQ$ control of the HKECS

Figure 4-6 shows the test results of the hardware paralleled emulators, as is shown a change of the phase injects some active power to the load. A change in the amplitude also injects some reactive power to the load, however it is shown how  $P$  and  $Q$  are tied together and are not controlled separately.

Various events are taken as following:

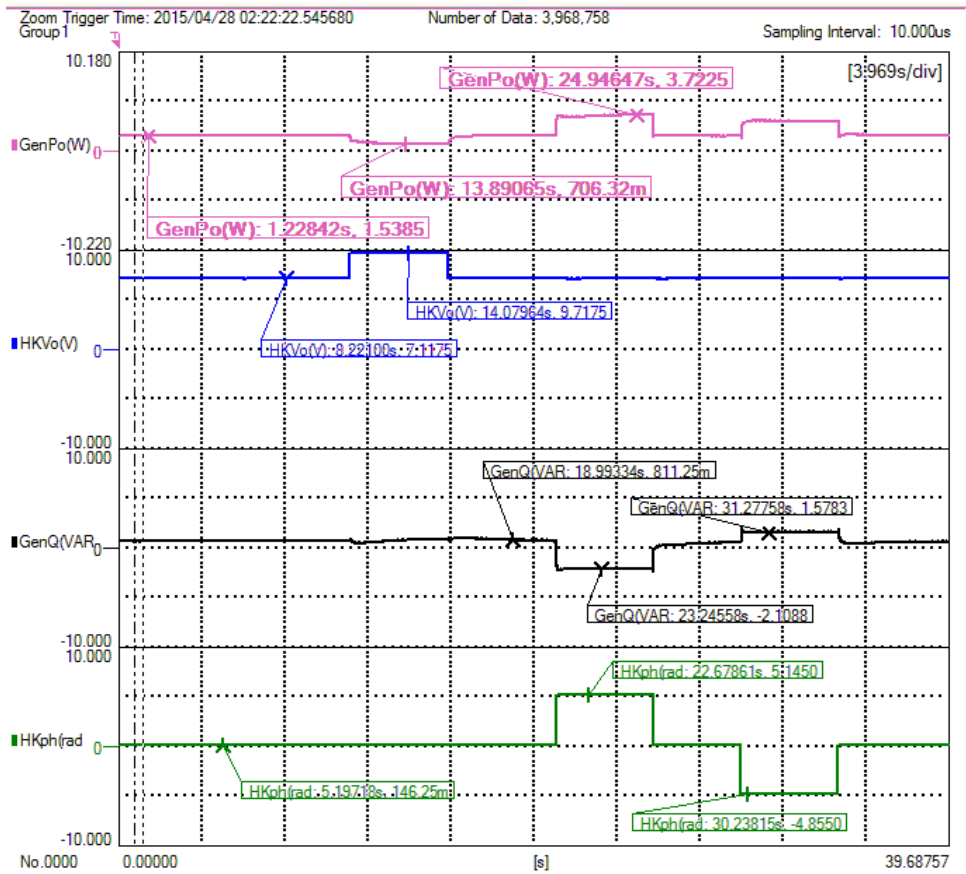


**Figure 4-6- From Top to Bottom: Generator output active power (Scale 1:350); HKECS output voltage level (scale 1:100); Generator output reactive power (Scale 1:350); HK source output voltage phase difference from genset(scale 1:36);**

- 1- At  $t=11$  Sec, the HKECS output voltage change from 70 V to 96 V. As is shown since the HKECS output reactive power increases, the Genset output power decreases to maintain the constant load power demand. P and Q components are shown how are tied together.
- 2- At  $t=22$  Sec the HKECS output voltage phase change from 0 degree to 90 degree. As is shown some active power is introduced in the genset output. Depending on the leading or lagging, Q is negative or positive.

#### 4.5.2. Decoupled PQ control of the HKECS

The decoupled PQ controller for the CCVSI which is discussed in “4.4.1” and “4.4.2” is designed for the HKECS. The CCVSI controller is configured for a decoupled PQ control and is connected in parallel with the grid (i.e. genset) for PQ control tests. Figure. 4-7

shows how the  $P$  and  $Q$  components of power are controlled individually. The droop factor is 2%,  $f_{NL} = 62 \text{ Hz}$ ,  $P_{Max} = 5 \text{ kW}$  ; and load changes from 660  $W$  to 910  $W$ .

Various events are taking place in the following order:

1. At  $t = 11 \text{ sec}$  the HKECS injects  $P = 400 \text{ W}$ .
2. At  $t = 21 \text{ sec}$  the HKECS injects no power
3. At  $t = 31 \text{ sec}$  the HKECS injects  $Q = 400 \text{ VAR}$ .
4. At  $t = 41 \text{ sec}$  the HKECS injects no power.
5. At  $t = 51 \text{ sec}$  the HKECS absorbs  $Q = 400 \text{ VAR}$ .
6. At  $t = 61 \text{ sec}$  the HKECS absorbs no power.
7. At  $t = 71 \text{ sec}$  the load is increased from 660  $W$  to 910  $W$
8. At  $t = 81 \text{ sec}$  the load is decreased from 910  $W$  to 660  $W$

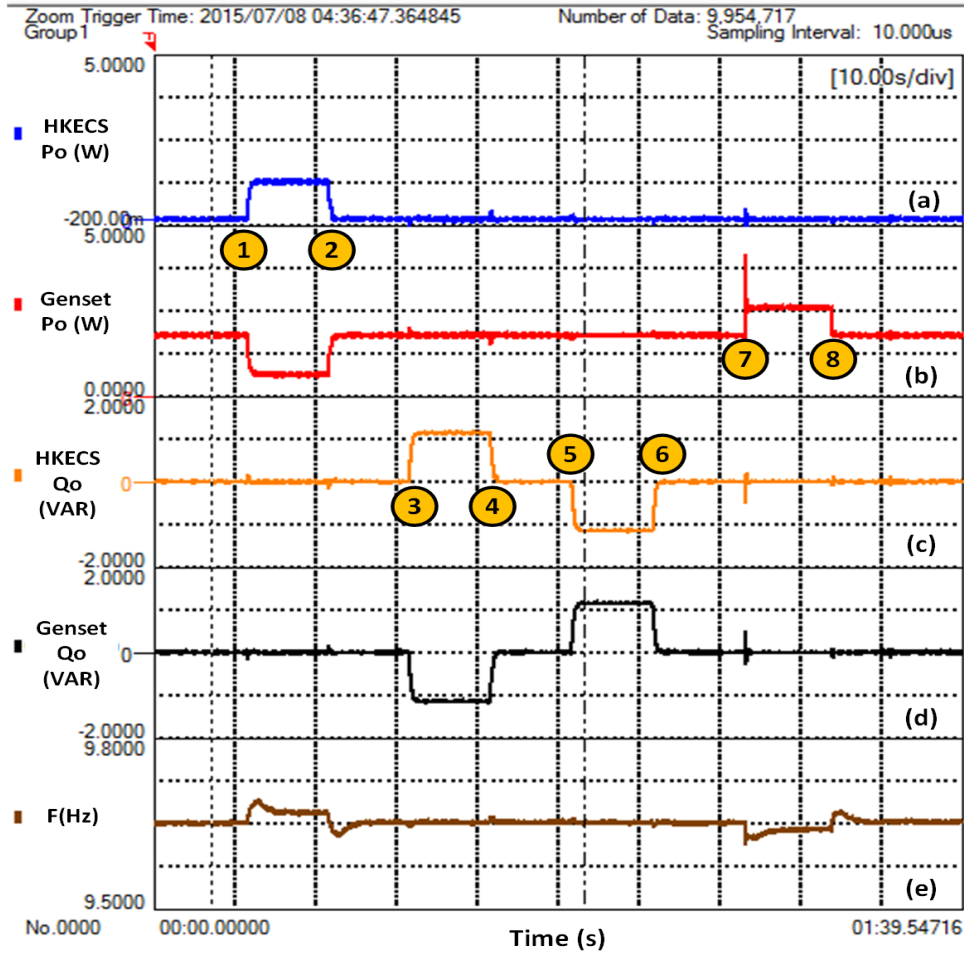


Figure. 4-7. Decoupled  $PQ$  sharing between genset and HKECS for a 2% frequency droop (a) HKECS output power (b) Genset output active power (c) HKECS output reactive power (d) genset output reactive power (e) Genset shaft frequency-there is an offset of  $-0.062V$  in the frequency curve. (Power scale: 350:1, Frequency scale:  $20/\pi$ :1).

Before the step No. 7, the load is a fixed value ( $660 W$ ) and power sharing is in a complementary fashion; at the point No. 7, the load is changed to  $910 W$  and the genset has picked up the extra load (since the HKECS is not injecting power any more) hence the frequency drops from  $61.83 \text{ Hz}$  to  $61.76 \text{ Hz}$  (there is an offset of  $-0.062V$  in the frequency curve). The frequency variations confirms the proper operation of the genset and the settling frequencies in the genset shown how the droop controller is functioning. As is shown a step change in  $P/Q$  does not affect the  $Q/P$  and powers are shared in a complementarily decoupled fashion. Frequency of the genset is only affected by injection or absorption of the  $P$  (and not  $Q$ ) which is because of using  $P$ - $f$  droop control.

#### **4.6. SUMMARY**

A CCVSI is designed and controlled as a decoupled PQ controller for being used as the HKECS steady state response emulations with certain assumption.

Both decoupled and coupled controlling methods are validated and compared experimentally.

#### **4.7. CONCLUSION**

The decoupled PQ controller shows independent control of the P and Q. the decoupled control of the P and Q are desired for the parallel operation of the HKECS. The Experimental validations show complementary load sharing between the genset and the HKECS emulators.

#### **4.8. CONTRIBUTIONS**

1. An active and reactive power general case decoupling method is proposed.
2. A CCVSI is designed to be employed as a decoupled PQ controller.
3. Some additional required equipment including voltage and current measurement devices and active filters are built for the feedback measurement of the CCVSI controllers.

### 5.1. INTRODUCTION

The distributed nature of different energy resources suggest the distributed power generation. If the power is to be generated from different sources, hence the power generators should operate in parallel. For the parallel operation of different generators such as HKECS and genset or multiple gensets some considerations should be taken.

The major reason for operating generators in parallel are:

1. The power demand exceeds the power output capability of one or more alternators.
2. From the economical point of view, alternators should be operated at the maximum efficiency. This is done by sharing the load among alternators.
3. Planned or emergency maintenance would be feasible in parallel operation.
4. Permits future expansion of the power generation and distribution.

Figure. 5-1 illustrates multiple genset operating in parallel.



**Figure. 5-1. Parallel placement of generators in a power generation utility**

As generator sets generate energy in parallel on the same load, they must be synchronised properly (voltage, frequency) and load distribution must be balanced properly. This function is performed by the regulator of each genset (thermal and excitation regulation).

The parameters (frequency, voltage) are monitored before connection: if the values of these parameters are correct, connection can take place.

## 5.2. CONSIDERATIONS FOR PARALLEL OPERATION

For parallel operation on the alternators, some considerations should be taken:

1. Synchronization
2. Load sharing
3. Protection

### 5.2.1. Synchronization

The alternators should be parallel through the circuit breaker switches and before the breakers connect the alternators together, the output voltages should be synchronized in the following manner:

1. The terminal voltages of the incoming alternator must be equal to the bus.
2. The frequency of the incoming alternator must be the same as the bus.
3. The phase and the sequence of phases should be the same.

Figure. 5-2 shows synchronization steps for two signals.

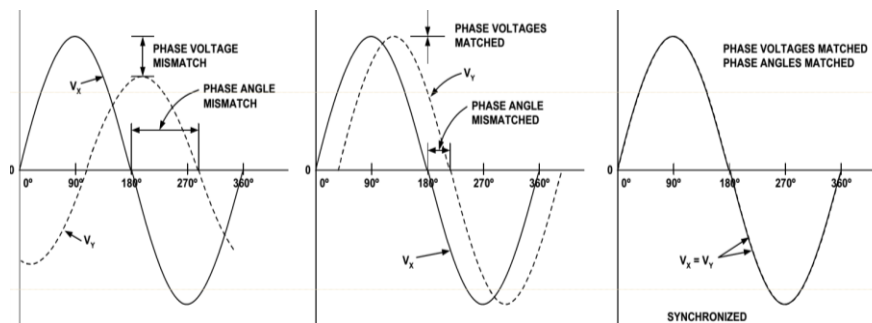


Figure. 5-2. Synchronization stages for two signals

Failure to meet any of the mentioned conditions an excessive circulating current could follow through the alternators.

The synchronization could be done with output signal comparisons using oscilloscope or a combination of synchronization lamp circuits and mustimeters.

### **5.2.2. Load Sharing**

Amount of the load could be shared un-symmetric with respect to the generators in a grid. Depend on the power rating and the other considerations including efficiency and cost per power production the load could be shared between sources un-symmetric.

For a proper load sharing, the alternators could sync the power demand through an additional “load demand bus” in isochronous mode or operating in droop controlled mode without the additional load demand bus.

In this thesis, the droop controlled mode which is well defined in the literature is employed and discussed in “1.3.4”, “1.3.5” and “4.4”.

### **5.2.3. Protection**

To avoid any fault transfer, reverse power and excessive circulating current in the parallel operation of the alternators, proper protection circuits should be designed.

Protection must respond to both system and microgrid faults. If the fault is on the utility grid, the desired response may be to isolate the microgrid from the main utility as rapidly as necessary to protect the microgrid loads. The speed of isolation is dependent on the specific customer s loads on the microgrid. In some cases sag compensation can be used without separation from the distribution system to protect critical loads. If the fault is within the microgrid, the protection coordinator isolates the smallest possible section of the radial feeder to eliminate the fault. Most conventional distribution protection is based on over current sensing. Power electronic based microsources cannot normally provide the levels of short circuit required to open breakers and blow fuses. Microsources may only be capable of supplying twice load, current or less to a fault. Some overcurrent sensing devices will not even respond to this level of overcurrent, and those that do

respond will take many seconds to respond, rather than the fraction of a second that is required [13].

### 5.3. EXPERIMENTAL VALIDATIONS

For experimental validations of output power sharing and frequency behaviour, parallel operation of a HKECS system with the genset emulator is verified. In this thesis the output voltage of the genset is kept constant, however a voltage droop can also be implemented to balance the reactive power based on the load sharing. The AVR can be controlled in such a way that removes this circulating power.

In the loading scenario, since the output power of the HKECS changes versus time, the diesel engine output power is controlled in such a way that compensate changes in the HKECS output power, supplying a constant power to the constant load. It is shown that the genset output power and frequency changes depending on the HKECS output power.

Various events which are taking place during the test are:

1. At  $t=5$  sec the HKECS injects 1kW power,  $P_{Load} = 1750 W$ .
2. At  $t=10$  sec the HKECS injects no power,  $P_{Load} = 1750 W$ .
3. At  $t=16$  sec the load is increased from 1750 W to 3200 W.
4. At  $t=24$  sec load is decreased to 1750 W.

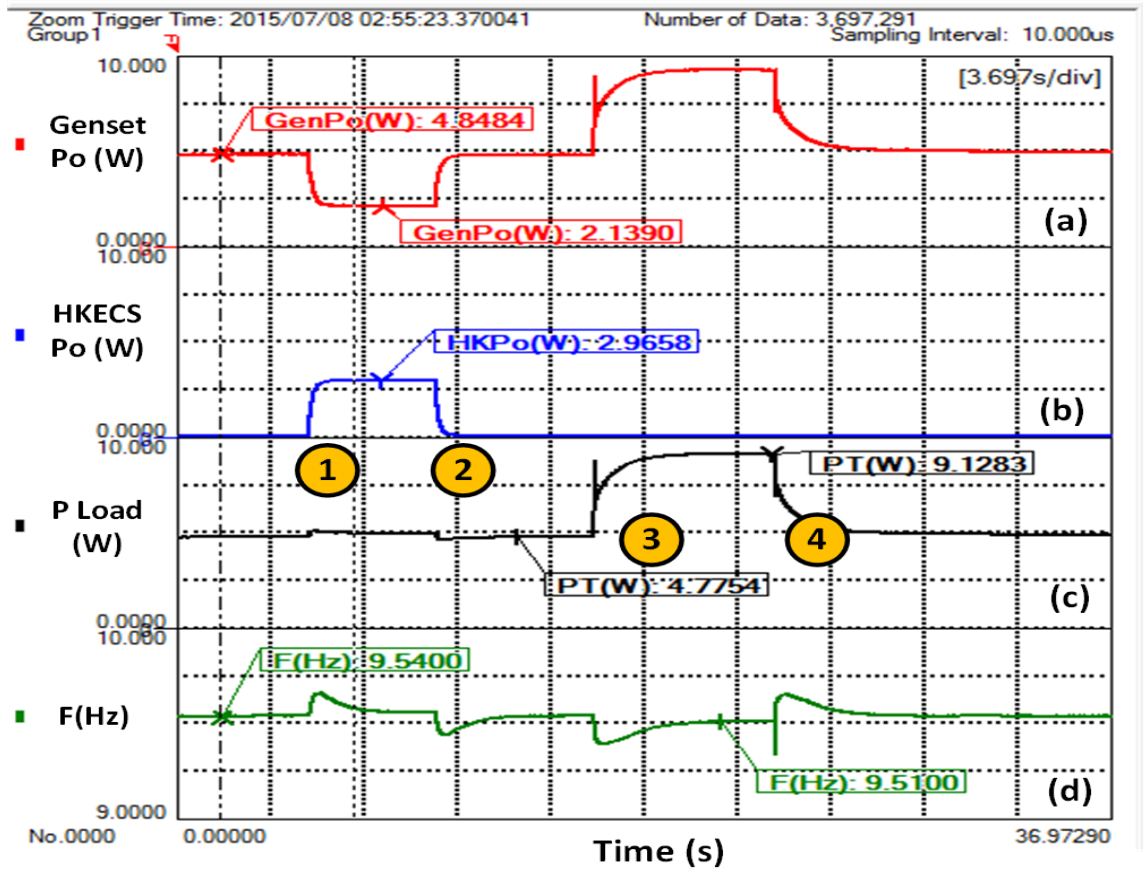


Figure. 5-3. Output power sharing and frequency of the parallel operation of the genset with a step power generation of a HKECS for 1% droop ( $f_{max} = 61 \text{ Hz}$ ,  $P_{max} = 5 \text{ kW}$ ). (a) Genset output power (b) HKECS generated power (c) Load power (d) Genset shaft frequency. (Power scale: 350:1, Frequency scale:  $20/\pi:1$ ).

It is shown that when the HKECS source injects some power to the grid, the genset supplies less power, the load is shared between sources and the output power is maintained constant (Figure. 5-3 (c) not including points 3 and 4). At  $t=16 \text{ sec}$  (point No. 3) the load is increased to show how does it affects the frequency and output power of the genset and it shows how the genset handles the additional required power. The frequency changes from 60.8 Hz to 60.54 Hz while the load changes from 1750 W to 3200 W. Figure. 5-3 (d) shows the transient changes in the frequency of the genset.

To investigate the behaviour of the emulator in parallel operation, a real case of the HKECS power flow is studied for a power plant [33] in the Point Evans, Washington;

and the power sharing results are shown in Figure. 5-4. For a better observation, the time scale of the power flow is changed from 24 hour to 24 seconds.

As is shown while the output power of the HKECS changes, power delivered to the load by the genset adapts to deliver a constant power to the load (Figure. 5-4 (c)). The genset output frequency also changes accordingly. It can be observed that at  $t=11.32$  sec, the maximum power is delivered by the HKECS which causes the genset to deliver the least power, hence the genset shaft speed and output frequency increases. The frequency changes from 60.98 Hz to 60.79 Hz while the HK power changes from 35 W to 770 W.

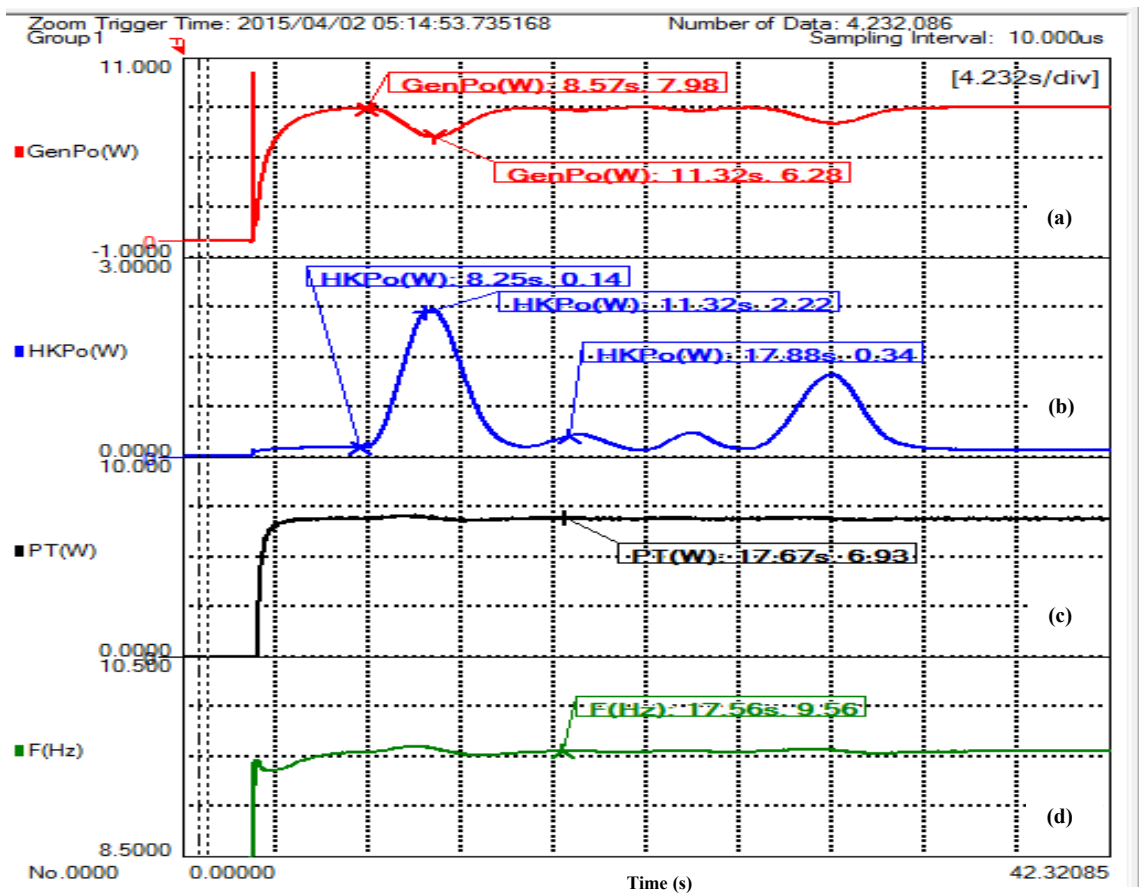


Figure. 5-4. Output power sharing and frequency of the parallel operation of the genset and a HKECS with a power profile of a power plant in Point Evans, for 2% droop ( $f_{max} = 61$  Hz,  $P_{max} = 5$  kW). (a) Genset output power (b) HK source generated power (c) Load power (d) Genset shaft frequency. (Power scale: 350:1, Frequency scale:  $20/\pi$ :1).

#### **5.4. SUMMARY**

Some considerations for the parallel operation of multiple generators and the genset are reviewed. The HKECS and genset emulators are connected in parallel with those considerations for the purpose of verifying the interaction between the genset and HKECS.

A real case water flow profile from a power plant in Point Evans in Washington is being used to verify the power profile of the emulator when the HKECS is being operated in a variable power profile as in real applications.

#### **5.5. CONCLUSION**

The output power sharing of the HKECS and the genset emulators are observed to behave in a complementary fashion which confirms the proper load sharing between the two generator emulators.

The frequency variations are observed to be within an acceptable range which confirm the proper operation of the droop controller that are employed in the control algorithms of the two emulators.

### 6.1. INTRODUCTION

Gensets are vastly used in remote areas where the wired electricity is not available or is not economically justified. Fuel transportation is costly and fuel cost itself is an issue in addition to the environmental impact of the genset including the heat and emission. For the above mentioned reasons, it is desirable to enforce the genset to operate at a specific operating point to satisfy (-some specific) ideal conditions. The ideal condition could be defined as any particular operating point in different terms including the BSFC, emission, efficiency etc., hence is called Ideal Operating Point (IOP) in this thesis. IOP is defined to happen at the minimum BSFC, Maximum efficiency or minimum emission.

As was discussed in Chapter 3. operating point of the genset regarding the BSFC, emission and efficiency are a function of the output power of the genset. In this chapter a novel method is introduced to track the IOP of the genset using a second generator (HKECS etc.) as a compensator through load sharing between genset and HKCES. Assuming the required amount of power is available to be delivered by the HKECS, the required power will be dictated by the genset through droop control to enforce the genset working around the IOP. The designed emulator is used to validate the proposed method experimentally.

### 6.2. GENERAL DESCRIPTION OF THE METHOD

Employing droop control, genset frequency varies depend on the applied load, hence operating point of the generator could be estimated through detection and analysis of the frequency. The idea is to inject the required power for compensation based on deviation of the frequency from an ideal value (e.g. 60Hz).

When using  $PQ$  control and AVR in the genset to control delivered power to the load, parallel operation of other sources of power (e.g. HKECS) affects the amount of the

power (hence frequency) delivered by the genset to the load in a complementary fashion as discussed in Chapter 5. If the HKECS increase the supplied power to the load, the output power delivered by the genset decreases and vice versa.

As is shown in 3, fuel consumption and emission of a genset varies with respect to its output power.

It is proposed in this chapter, that the amount of the power provided by the HKECS be controlled in such a way to keep the genset in a particular operating point in terms of its output power, efficiency, emission or fuel consumption. Since the load and demanded power can vary, it is required to determine and communicate between two sources how much power is needed from the HKECS to keep the genset in the ideal operation without any additional communication channel. A droop control method can be configured to set the output frequency of the genset according to the demand operating point as an indirect communication method.

### **6.3. A MODIFIED DROOP CONTROL SCHEME FOR IOP TRACKING OF THE GENSET**

Voltage and frequency droop controllers are well defined in the literature and are explained in section 1.3.4 and 1.3.5. In frequency droop control, the output frequency varies with the output power linearly. In a similar way, the output frequency can be defined to vary according to the other characteristic (BSFC, Emission, etc.) rather than output power.

Using power-frequency ( $P-F$ ) droop control for the genset, the amount of the power delivered to the load by genset can be detected by HKECS side through analysing the frequency; but to find the IOP of a specific genset, the power-operating map of that individual genset should be known and programmed in to the HKECS. It is cumbersome to meet this essential requirement and definition of such map is not desirable and practical in real application.

As is proposed in this thesis, to enforce the genset in the IOP and to eliminate necessity of defining the power map of the genset to the second source (e.g. HKECS) with the purpose of achieving a plug and play configuration, the operating point condition (BSFC, etc.) of the genset is used instead of the delivered power of the genset in droop control. The  $P$ - $F$  droop scheme is proposed to be modified to reflect the operating point of the system in terms of frequency. The IOP can be defined in terms of emission, efficiency, BSFC in droop curve.

In other words, instead of the reflection of the operating point in the power and from the power to the frequency, operating point (i.e. deviation from IOP) can be mapped into the frequency directly as is shown in Figure. 6-1:

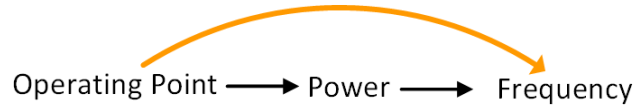


**Figure. 6-1. Direct operating point mapping to the frequency**

In this thesis, reference frequency of the genset would vary according to the BSFC, and the HKECS (or any other parallel source) could determine the amount of the power required to enforce the genset into the IOP through analysing the frequency and trying to keep the operating frequency close to the IOP frequency (e.g. 60 Hz) using a PI controller. In other words, the deviation from the IOP in the genset would be detected and compensated with the HKECS. Assuming the IOP in a particular genset happens at the base frequency as is shown in Figure. 6-2, for a genset operating at the output power of  $P$ , the output frequency (which contains IOP information) with a linear droop is:

$$f_{gen} = m \times (P - P_{IOP}) + f_{IOP} \quad (6.1)$$

$$m = \frac{f_{min} - f_{NL}}{P_{full}} = -D \times \frac{f_{IOP}}{P_{full}} \quad (6.2)$$

where the  $P_{IOP}$  is the power at which the genset operates ideally,  $f_{IOP} = f_{base}$  is the base frequency which the genset can be set to work at the IOP,  $D$  is the droop percent typically less than 5%, and  $P_{full}$  is the genset full load power.

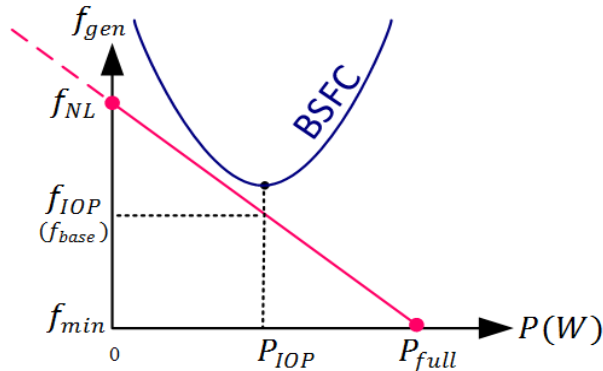


Figure. 6-2. Linear droop scheme for a genset to reflect IOP (BSFC in this case) in frequency (i.e. to map the BSFC into the power)-the base frequency of 60 Hz happens at IOP in a particular genset.

### 6.3.1. The Real Case

If IOP does not happen at the base frequency (as in most of the cases in real applications) droop line can be shifted so that genset operates at the base frequency while supplying the IOP power as is shown in Figure. 6-3. This can be done by adjusting the no load frequency.

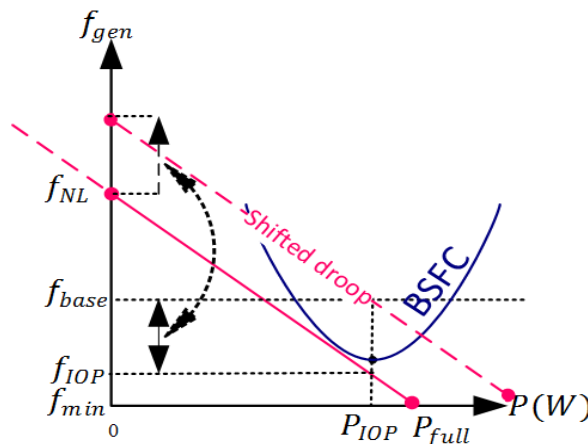


Figure. 6-3. Linear droop scheme for a genset to reflect IOP (BSFC in this case) in frequency- a case in which the IOP is not happening at the base frequency; Droop line is shifted to force  $f_{IOP} = f_{base}$ .

Equation (6.1) and (6.2) represent linear droop definition for the IOP in terms of BSFC as is shown in Figure. 6-2 (a) while the IOP is defined to happen at minimum BSFC.

Some percentage of the normalized characteristic curve of the genset (BSFC, etc.) is suggested to be multiplied with the linear droop line to modulate frequency in such to reflect operating condition of the genset (BSFC, etc.) in the frequency. In this case, (if required) it is possible to detect the exact BSFC curve of the genset without requiring any additional data transfer (e.g. in the HKECS side if is required in any applications) through monitoring the bus frequency by applying a linear power sweep load anywhere in the grid. Experimental tests for this method is provided in Figure. 6-7.

Consequently, droop for the genset reflecting BSFC is to be defined in the following manner:

$$f(P)_{mod} = (f(P)_{lin} - f_{IOP}) \times (BSFC(P)_{Norm}) + f_{IOP} \quad (6.3)$$

$$BSFC(P)_{Norm} = \left( \frac{(1 - p) + p(BSFC(P) - BSFC_{IOP})}{BSFC_{max} - BSFC_{IOP}} \right) \quad (6.4)$$

where  $f(P)_{lin}$  is the linear droop line function ( $f_{gen}$ ) defined in (25),  $f_{IOP}$  is the frequency at which the genset is in IOP,  $BSFC(P)_{Norm}$  is the normalized BSFC curve,  $p$  is the modulation index percentage,  $BSFC_{IOP}$  is the BSFC value at the IOP,  $BSFC_{max}$  is the maximum BSFC.

Value of the  $p$  could be determined based on the dynamics and response time of the generators and is a value from 0 to 1. As  $p \rightarrow 0$ , the droop line converges to a linear droop line; for  $p = 1$ , the droop line more reflects the effect of the BSFC curve. Depending on the BSFC curve, bigger values of  $p$  typically causes less frequency variations around IOP when the output power changes; which causes the power sharing being more sensitive to the frequency variations.

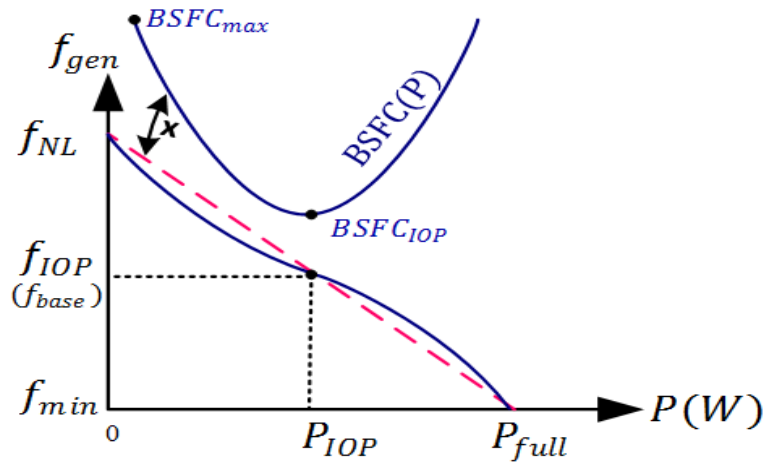


Figure. 6-4. A sample modified droop line with 40% ( $p = 0.4$ ) effect of normalized BSFC curve to reflect the BSFC in the frequency.

#### 6.4. COMPENSATION OF THE POWER

On the HKECS side, the controller should be programmed to bring the operating frequency of the system back to the  $f_{IOP}(= f_{base})$  value (e.g. 60 Hz) when the load changes through injecting or consuming some power to keep the genset operating at IOP. Assuming that there is enough power available in the HKECS side, if  $f_{gen} < f_{IOP}$ , HKECS increases its injected power which causes the operation frequency increase back to the ideal point; on the contrary if  $f_{gen} > f_{IOP}$  the injected power could decrease or some power could be consumed; the amount of energy can be stored in the battery or to the water through heating and can be used for residential demand. A simple PI controller could be designed to control HKECS for this purpose. The input to the controller is the bus (i.e. genset) frequency and the controlling parameter is the active power ( $P$ ).

The PI controller on the HKECS side to track the IOP is designed with the Ziegler-Nichols Method, the stability analysis and more precise controller are recommended for the future work.

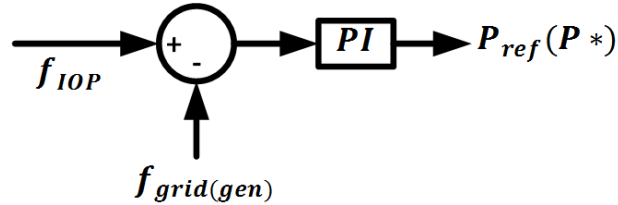


Figure. 6-5. Frequency control of the grid through power delivery .

For the compensation of the power on the HKECS side it is assumed that the load power does not exceed the maximum available power of the HKECS.

## 6.5. EXPERIMENTAL VALIDATIONS

### 6.5.1. Linear Droop

Value of the droop is typically between 1% and 5%. For the experimental results the average value of 3% is chosen.

For experimental validations, the method with a linear droop of 3% with  $f_{NL} = 61.2$  Hz,  $P_{max} = 1200$  W (Figure. 6-6) and the modified droop based on the BSFC with  $f_{NL} = 62$  Hz (Figure. 6-7) is implemented to enforce the genset to work at the IOP. The BSFC curve shown in Figure. 3-1 is scaled for the power rating from 200 W to 1200 W. Results are shown in Figure. 6-6 and Figure. 6-7.

Various events are taking place during the test in the following order:

1. At  $t = 3$  sec load increases linearly from  $P = 220$  W to 1200 W to show how BSFC changes vs  $P$ .
2. At  $t = 23$  sec the load stops changing.
3. At  $t = 30$  sec the HKECS gets connected to the bus through the circuit breaker and starts injecting.
4. At  $t = 34$  sec HKECS brings the genset back to the IOP by injecting  $P = 350$  W.
5. At  $t = 43$  sec the load increases from  $P = 1200$  W to  $P = 2000$  W and HKECS starts to handle the extra power.
6. At  $t = 47$  sec HKECS brings the genset back to the IOP by injecting  $P = 800$  W.

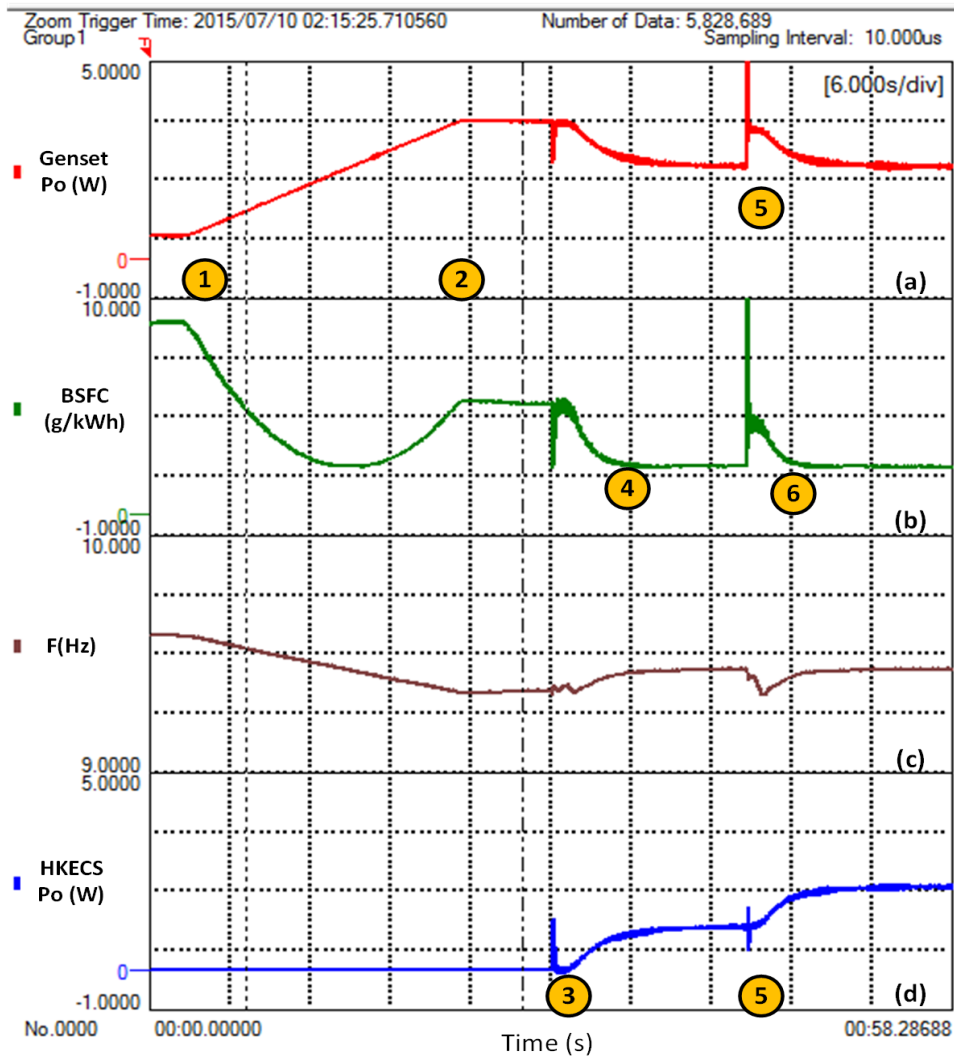


Figure. 6-6. Enforcing genset to the IOP using linear droop control scheme by HKECS. (a) The genset output power (b) Scaled BSFC of the genset in Figure. 3-1 (c) Bus frequency with a linear 3% droop (d) The HKECS output power (Power scale: 350:1, Frequency scale:  $20/\pi$ :1, BSFC scale: 80:1).

As can be observed, the BSFC of the genset changes versus power according to the Figure. 3-1, while the  $P_{max}$  for the genset is scaled for 1200 W. Droop percentage is defined to insure that genset and HKECS are at the rated power when operating at the minimum frequency.

It is shown how the HKECS compensates the load and brings the genset back to the IOP to consume less possible fuel per generated output power (point No. 4 and No. 6 in

Figure. 6-6). In other word, the HKECS forces the BSFC to its minimum value. Amount of the fuel saving according to a sample BSFC Figure. 3-1 (b) for a load with  $P = 1200 W$  is:

$$BSFC_1 = 5.25 \times 80 = 420 \frac{gr}{kWh} \quad (6.5)$$

$$BSFC_2 = 2.25 \times 80 = 184 \frac{gr}{kWh} \quad (6.6)$$

$$Fuel\ consumption_1 = (BSFC_1 \times \int P_1 \times dt = (5.25 \times 80 \times 1.2kW) \times \frac{17}{60 \times 60} = 2.38\ gr \quad (6.7)$$

$$Fuel\ consumption_2 = (BSFC_2 \times \int P_2 \times dt = (2.25 \times 80 \times 0.84kW) \times \frac{17}{60 \times 60} = 0.71\ gr \quad (6.8)$$

$$Fuel_{saved} = Fuel\ consumption_2 - Fuel\ consumption_1 = 1.65\ gr \quad (6.9)$$

$BSFC_1$ : BSFC of the genset before compensation

$BSFC_2$ : BSFC of the genset after compensation

Amount of the fuel saved in this mode is approximately 1.7 gr in 17 seconds (about 1 gr in 10 seconds or 6 gr/min).

It should be noted that there is an assumption that the HKECS available power is less than the total required power of the load. (i.e.  $P_{HKECS} < P_{LOAD}$ ,  $P_{gen} > 0$ ). Otherwise if the total power could be produced only with the HKECS, the entire load could be handled by HKECS.

It should also be noted that, if the HKECS is not injecting the maximum available power, thus enforcing the genset to work at the IOP with the minimum BSFC, it does not mean that the less possible fuel is consumed by the genset, however in this experiment the purpose is to show how to enforce the genset to work at a particular (IOP) operating point. If the method being adjusted based on the other desired parameters (e.g. minimum

emission, etc.) rather than minimum BSFC, the HKECS would be used to achieve the related condition (Minimum emission, etc.).

There are some advantages when the genset is forced to operate at the minimum BSFC. Most importantly, the ICEs are designed to have the best performance around the minimum BSFC point. Consequently the maintenance and other infrastructure cost would be decreased.

In case which the HKECS injects the maximum power using MPPT, then obviously the less possible fuel will be consumed, however it causes the genset not to operate at the IOP. In this case from Figure. 6-6, amount of the fuel used for the previous scenario would be:

$$Case\ 1 = (BSFC_{c1} \times \int P_1 \times dt = (3.62 \times 80 \times 0.525kW) \times \frac{17}{60 \times 60} = 0.718\ gr \quad (6.10)$$

$$Case\ 2 = (BSFC_{c2} \times \int P_2 \times dt = (2.25 \times 80 \times 0.84\ kW) \times \frac{17}{60 \times 60} = 0.714\ gr \quad (6.11)$$

$$\%Increased\ Fuel = \frac{0.714 - 0.718}{0.718} = -0.56\% \quad (6.12)$$

*Case 1:* Fuel consumption in 17 sec when HKECS injects the maximum power.

*Case 2:* Fuel consumption in 17 sec when HKECS injects the required power to track IOP.

As is shown from (6.12), when the HKECS operates to enforce the genset to work at the IOP, it even decrease the fuel consumption of the genset by 0.56% in comparison to when the HKECS injects the maximum power (e.g. using MPPT). In addition, operating at the IOP brings other advantages such as increasing the lifetime of the genset and decrease the maintenance cost of the genset. It should also be noted that the calculations in (6.5) to (6.12) are based on an assumed BSFC curve. Depend on the BSFC in the real applications the method could increase or decrease the fuel consumption.

### 6.5.2. Modified Droop

In Figure. 6-6 is shown how frequency changes linearly versus power because of using a linear droop. In contrast, frequency in Figure. 6-7 is shown how it changes according to the BSFC as is discussed in “6.3.1” this also causes having less converge time for the frequency (2.4 sec in Figure. 6-7 (c) instead of 4 sec in Figure. 6-6 (c)). More investigations are required to explain details which is recommended for the future work. In contrast with linear droop test, in this test HKECS is not injecting power with MPPT.

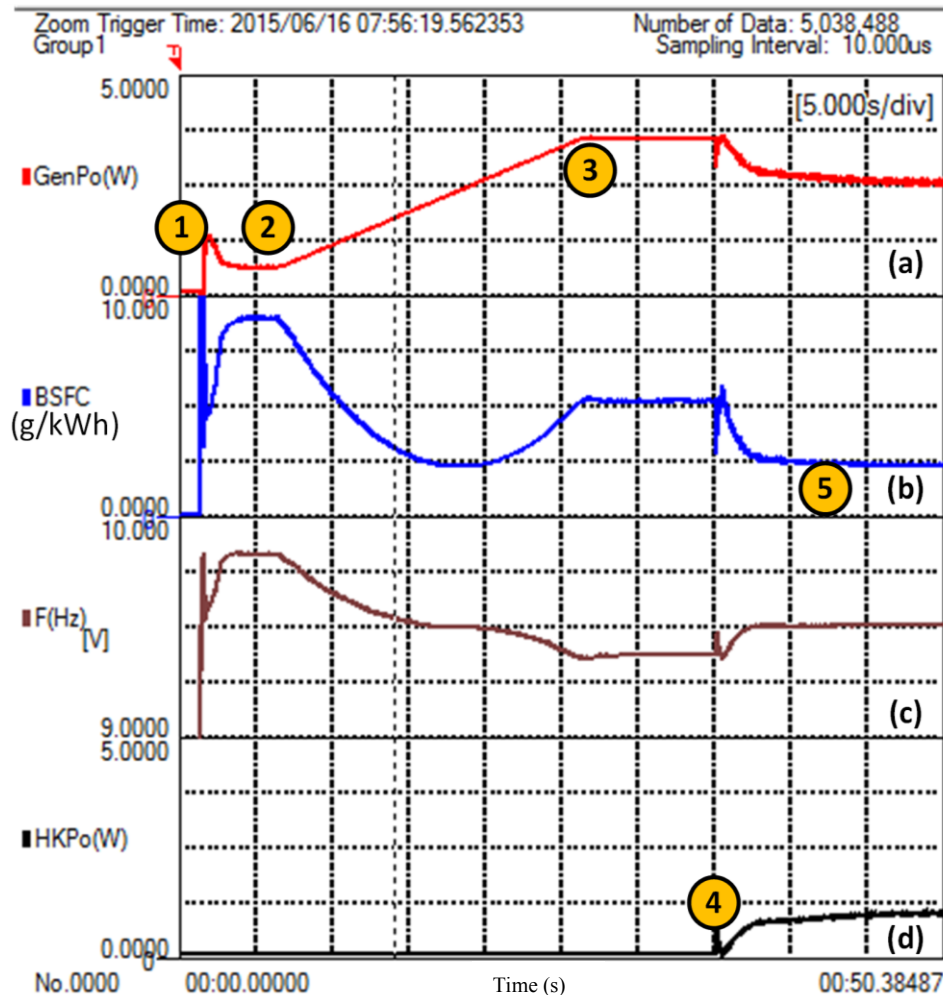


Figure. 6-7. Enforcing genset to the IOP using modified droop control scheme by HKECS. (a) The genset output power (Power scale: 350:1) (b) Scaled BSFC of the genset in Figure. 3-1 (BSFC scale: 80:1) (c) Bus frequency modified droop based on BSFC (Frequency scale:  $20/\pi$ :1) (d) The HKECS output power (Power scale: 350:1).

The value of  $p = 0.4$  is considered to be suitable for the experimental setup to avoid the power sharing being sensitive to the frequency variations.

In a similar way the same power management strategy could be used to enforce the genset to operate in the maximum efficiency or less possible emission by setting the ideal operating frequency based on the desired parameter instead of the BSFC.

Various events are taking place during the test in the following order:

7. At  $t = 6 \text{ sec}$  load increases linearly from  $P = 220 \text{ W}$  to  $1200 \text{ W}$  to show how BSFC changes vs  $P$ .
8. At  $t = 26 \text{ sec}$  the load stops changing.
9. At  $t = 36 \text{ sec}$  the HKECS gets connected to the bus through the circuit breaker and starts injecting.
10. At  $t = 38.4 \text{ sec}$  HKECS brings the genset back to the IOP by injecting  $P = 350 \text{ W}$ .

Amount of the fuel saving according for this scenario is:

$$BSFC_1 = 5.2 \times 80 = 416 \frac{gr}{kWh} \quad (6.13)$$

$$BSFC_2 = 2.3 \times 80 = 184 \frac{gr}{kWh} \quad (6.14)$$

$$Fuel\ consumption_1 = (BSFC_1 \times \int P_1 \times dt = (5.2 \times 80 \times 1.2kW) \times \frac{17}{60 \times 60} = 2.35 \text{ gr} \quad (6.15)$$

$$Fuel\ consumption_2 = (BSFC_2 \times \int P_2 \times dt = (2.3 \times 80 \times 0.91 \text{ kW}) \times \frac{17}{60 \times 60} = 0.79 \text{ gr} \quad (6.16)$$

$$Fuel_{saved} = Fuel\ consumption_2 - Fuel\ consumption_1 = 1.5 \text{ gr} \quad (6.17)$$

$BSFC_1$ : BSFC of the genset before compensation

$BSFC_2$ : BSFC of the genset after compensation

As was expected in (6.17), amount of the fuel consumption is not changed noticeably in compare with the linear droop scenario.

## **6.6. SUMMARY**

A new method is proposed to enforce the genset to operate at the IOP. Two different types of the method (using linear and a modified droop controllers) are implemented and the experimental validations are conducted to validate the overall improvement of the genset operation.

The method is implemented to yield the best operating point of the genset in terms of the BSFC. It is discussed how to achieve improvements in the efficiency and emission improvements using the same concept.

A frequency controller on the HKECS is proposed for IOP tracking of the genset using certain assumptions.

## **6.7. CONCLUSIONS**

The experimental validations show a decrease in the fuel consumption about 6 gram per minutes for an assumed sample BSFC curve for a genset with a different power scale.

The modified droop control method shows shorter frequency convergence time in compare with the linear droop control. The detailed analysis is recommended for as the future works.

## **6.8. CONTRIBUTIONS**

1. A novel methods to enforce the genset to operate in the ideal operating point (IOP) which could be defined based on the minimum BSFC, maximum efficiency or minimum emission is proposed. IOP tracking based on the minimum BSFC is studied in the thesis. The method does not require additional communication channel and detects the operating point based on the frequency behaviour.
2. A new method to detect BSFC curve of the genset without using an extra communication channel using droop control method is provided.

### 7.1. SUMMARY

A diesel engine generator set (genset) is emulated using power electronic devices and mathematical models of different parts in a typical genset are used to be included in the control algorithms.

The thesis is defined to make a system (an emulator) which generate the same transient and steady state response as in a real genset. A VSI with current and voltage control loops is designed and controlled with some reference signals to produce the same output as in a real genset. Reference signals for the VSI are the output of the SG model-(driven by the engine and coupling shaft model). Having the input torque and speed of the engine, the output generated voltage signal of the SG is known which feeds the VSI to generate the output voltage; which makes an emulated version of the genset.

The controller and peripheral algorithms are implemented in Simulink and are compiled to the DS-1103 dspace controller and a hardware setup is built to verify the emulator response. It is shown that when the load or input power changes how the transient and steady state responses (due to the SG and ICE inertia and time delay and other characteristics of a typical genset) are compatible with a commercial gensets which are provided in some paper publications.

Another version of the hardware setup is prepared and reconfigured to implement a HKECS for the parallel operation with the genset. The parallel operation is studied and different tests are conducted to verify the interaction of the sources. The emulation of the genset has led to a novel method to enforce the genset to work with the least fuel consumption per generated output power and the idea is implemented and tested for verification.

## 7.2. CONCLUSION

To conclude, the steady state and transient response of the emulated genset are compared with the other publications which confirms the compatibility of the responses with the other publications results. The emulator is designed in a reconfigurable manner using not only a solid hardware but also control algorithm defined in the software which facilitates emulation of the similar power generators, for instance HKECS, wind generators, etc.

A parallel operation of the genset with the HKECS is verified and the coupled and decoupled control of active and reactive powers are carried out which show how a CCVSI can control or compensate active or reactive power individually.

A novel idea is proposed to enforce the genset to work at a certain operating point called IOP, to have a genset with the less emission, more efficient and less fuel consumption per unit generated output power. The algorithm is included in the genset emulator and results show improvements in fuel consumption for a specific BSFC curve approximately 1 *gr* in 10 seconds for a load of  $P=1200$  W using the proposed method.

## 7.3. FUTURE WORKS

Following are the most important recommended works to do in the future:

1. The frequency PI controller on the HKECS side to track the IOP is designed with the Ziegler-Nichols Method, the stability analysis and more precise controller design could be carried out.
2. The IOP tracking of the genset is defined for the BSFC in the thesis. It is recommended to design the similar approach for the IOP tracking based on optimizing the emission and/or efficiency.
3. Effect of the modified droop instead of a linear droop on the performance of the system could be investigated in more details.
4. Since there are some similarities, the emulator could be reconfigured to emulate series-HEV and wind turbine generator.

# APPENDIX A

The transfer function (average model) for a grid tied VSI shown in Figure. A-7-1 is well defined in the literature as [34]:

$$\frac{v_{RL}(s)}{V_{ctrl}(s)} = \frac{v_a}{v_{tri}} \frac{1}{sL + R} \quad (A.1)$$

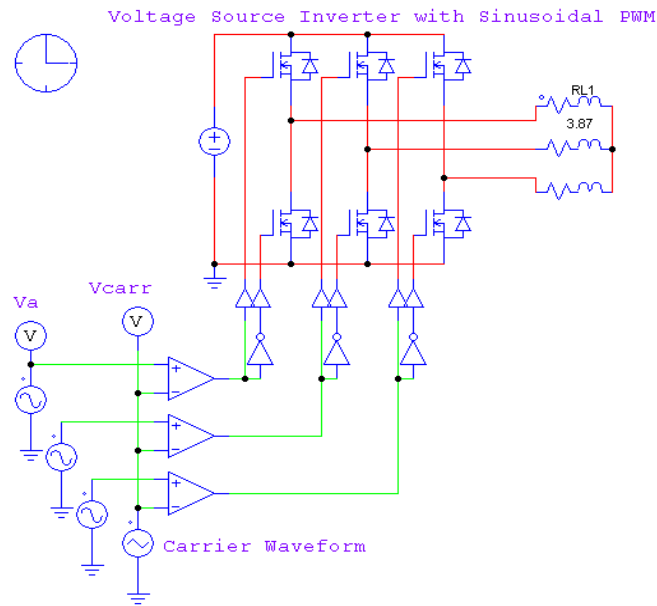


Figure. A-7-1. Schematic diagram of a grid connected VSI.

Form of the transfer function (A.1 and Figure. A-7-2) suggests using a type-2  $P$  controller.

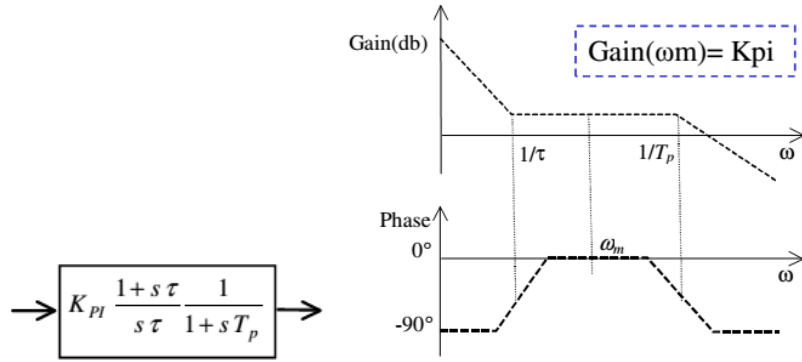


Figure. A-7-2. Type-2 PI controller [35].

To design the controller, gain ( $P$ ) at the  $\omega_m$  frequency should be defined so that the net gain at that frequency be equal to 1 (i.e.  $P = 1/K_{pi}$ ).

Amount of the required phase boost can be obtained from (A.1) at the  $\omega_0 = 60 \text{ Hz}$  to form a phase shift between  $\phi = 40^\circ \sim 60^\circ$ .

$$\phi = -90 + \text{boost} \quad (0^\circ < \text{boost} < 90^\circ) \quad (\text{A.2})$$

$$K = \tan\left(\frac{\text{boost}}{2} + 45^\circ\right) \quad (\text{A.3})$$

And controller parameters ( $\tau$  and  $T_p$ ) would be:

$$\tau = \frac{K}{\omega_m} \quad (\text{A.4})$$

$$T_p = \frac{1}{K\omega_m} \quad (\text{A.5})$$

Electric circuit shown in Figure. A-7-3 could be used as the controller in case of hardware control.

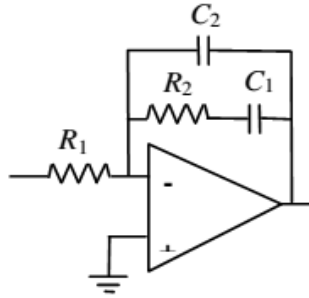


Figure. A-7-3. Schematic diagram of a grid connected VSI [35].

$$\tau = R_2 C_1 \quad (\text{A.6})$$

$$T_p = R_2 \frac{C_1 C_2}{C_1 + C_2} \quad (\text{A.7})$$

$$K_{pi} = -\frac{C_1 R_2}{R_1 (C_1 + C_2)} \quad (\text{A.8})$$

# APPENDIX B

TABLE I-SPEED GOVERNOR AND AVR CONTROLLER SET PARAMETERS

<i>Parameter</i>	<i>Value</i>	<i>Parameter</i>	<i>Value</i>
$k_{pG}$	5.6e-3	$k_{pAVR}$	0.305
$k_{iG}$	0.0064	$k_{iAVR}$	1.782
$k_{dG}$	639e-4	$k_{dAVR}$	6e-3

TABLE II-VSI CONTROLLER SET PARAMETERS (5 kVA, 110 V, 60 Hz)

<i>Parameter</i>	<i>Value</i>	<i>Parameter</i>	<i>Value</i>
$F_s$	6 kHz	$k_{pvq}$	1.8
$L_f$	24 mH	$k_{ivq}$	189
$C_f$	110 $\mu$ F	$k_{dvq}$	0.001
$F$	0.6	$k_{pid}$	0.17
$k_{pvd}$	1.8	$k_{iid}$	0.005
$k_{ivd}$	189	$k_{did}$	0.001
$k_{avd}$	0.001	$k_{piq}$	0.17
$F_{-3db\ filt\_abc}$	180 Hz	$k_{iiq}$	0.005
$F_{-3db\ filt\_dq}$	18 Hz	$k_{diq}$	0.001

TABLE III-CCVSI CONTROLLER SET PARAMETERS (5 kVA, 110 V, 60 Hz)

<i>Parameter</i>	<i>Value</i>	<i>Parameter</i>	<i>Value</i>
$F_s$	6 kHz	$k_{pid}$	6
$L_f$	24 mH	$k_{iid}$	213
$F_{-3db\ filt\_abc}$	180 Hz	$k_{piq}$	6
$F_{-3db\ filt\_dq}$	34 Hz	$k_{iiq}$	213
$Z_{coupling}$	4.5 $\Omega$		

TABLE IV-PQ CONTROLLER SET PARAMETERS

<i>Parameter</i>	<i>Value</i>	<i>Parameter</i>	<i>Value</i>
$k_{pp}$	0.35	$k_{pq}$	0.35
$k_{ip}$	1.4	$k_{iq}$	1.4
$k_{dp}$	0.00001	$k_{dq}$	0.00001

TABLE V-FREQUENCY COMPENSATOR CONTROLLER SET PARAMETERS

<i>Parameter</i>	<i>Value</i>	<i>Parameter</i>	<i>Value</i>
$k_{pf}$	2	$k_{if}$	263

TABLE VI-DIESEL ENGINE PARAMETERS

<i>Parameter</i>	<i>Value</i>	<i>Parameter</i>	<i>Value</i>	<i>Parameter</i>	<i>Value</i>
$k_e$	60e3	$t_d$	22e-3	$t_e$	0.1

TABLE VII-SYNCHRONOUS MACHINE PARAMETERS

<i>Parameter</i>	<i>Value</i>	<i>Parameter</i>	<i>Value</i>
$P_{nom}$	20 kVA	$R_s$	1.6 $\Omega$
$V_{nomll}$	230 V	$L_l$	4.56 mH
$F_{nom}$	60 Hz	$L_{md}$	108.6 mH
<i>Inertia</i>	0.0923 $k_s$	$L_{mq}$	51.6 mH
<i>Friction</i>	0.0125 N	$R_F$	1.16 $\Omega$
<i>Pole pairs</i>	2	$L_F$	11.4 mH
$R_{kd}$	3.66 $\Omega$	$L_{kd}$	9.16 mH
$R_{kq}$	4.75 $\Omega$	$L_{kq}$	10.06 mH

# REFERENCES

- [1] M., Dalal-Bachi, "Economic dispatch and demand side management in diesel hybrid mini-grids." M.S. thesis, ECE. Dept., Concordia Univ., MTL., QC, 2012.
- [2] P., Piagi, Lasseter, R.H., "Autonomous control of microgrids," in Power Engineering Society General Meeting, Montreal, 2006.
- [3] Salehi, V., Mohamed, A., Mazloomzadeh, A., Mohammed, O.A., "Laboratory-Based Smart Power System, Part I: Design and System Development," Smart Grid, IEEE Transactions on, vol. 3, no. 3, pp. 1394-1404, 2012.
- [4] J. Jeon, J. Kim, H. Kim, S. Kim, Changhe, "Development of Hardware In-the-Loop Simulation," Power Electronics, IEEE Transactions on, vol. 25, no. 12, pp. 2919-2929, 2010
- [5] R. Lasseter, "Smart Distribution: Coupled Microgrids," Proceedings of the IEEE, vol. 99, no. 6, pp. 1074-1082, 2011.
- [6] J. R. K. Neely, R. Jepsen, J. Roberts, S. Glover, F. White and M. Horry, "Electromechanical emulation of hydrokinetic generators for renewable energy research," in Oceans - San Diego, 2013 , San Diego, CA, 2013 .
- [7] J.C. Neely and S. Pekarek, S. Glover, Finn, J., Wasynczuk, O, "An economical diesel engine emulator for micro-grid research," in Power Electronics, Electrical Drives, Automation and Motion (SPEEDAM), 2012 International Symposium on, Sorrento, 2012.
- [8] L. L. Torres, M. , "Inverter-based virtual diesel generator for laboratory-scale applications," in IECON - 36th Annual Conference on IEEE Industrial Electronics Society, Glendale, AZ, 2010.
- [9] L. A. C. L. Miguel Torres, "Inverter-Based Diesel Generator Emulator for the Study of Frequency Variations in a Laboratory-Scale Autonomous Power System," Energy and Power Engineering, vol. 5, no. 3, pp. 274-283 , 2013.
- [10] I. Husain, (2010). Electric and Hybrid Vehicles: Design Fundamentals, Second Edition. CRC Press.
- [11] P.H., Bauer, Q.T Bui, (2013). On the optimal choice of operating points in large series hybrids. Electric Vehicle Symposium and Exhibition (EVS27) (pp. 1-5). Barcelona: IEEE.

- [12] S., Overington, & Rajakaruna, S. (2014). "A novel model of internal combustion engine for high efficiency operation of hybrid electric vehicles and power systems." Power Engineering Conference (AUPEC), 2014 Australasian Universities , (pp. 1-6). Perth, WA.
- [13] R. Lasseter, "Microgrids" Power Engineering Society Winter Meeting, 2002. IEEE, vol. 1, no. 6, pp. 305-308, 2002.
- [14] S. Krishnamurthy, T.M Jahns, R.H., Lasseter, "The operation of diesel gensets in a CERTS microgrid," in Power and Energy Society General Meeting - Conversion and Delivery of Electrical Energy in the 21st Century, Pittsburgh, PA, 2008.
- [15] L. A. C. L. Miguel Torres, "Dynamic Frequency Control in Diesel-Hybrid Autonomous Power Systems using Virtual Synchronous Machines" PhD. thesis, ECE. Dept., Concordia Univ., MTL., QC, 2013.
- [16] I. Boldea, The electric generators handbook, Variable Speed Synchronous Generators, Boca Raton: CRC Press, 2006.
- [17] R. A. Pearman, Electrical machinery and transformer technology, Philadelphia: Saunders College Publishing, 1994.
- [18] I. Boldea, Synchronous Generators Handbook,, Boca Raton: CRC Press, 2006.
- [19] S. Roy, O. Malik and G. Hope, " A least-squares based model-fitting identification technique for diesel prime-movers with unknown dead-time," Energy Conversion, IEEE Transactions on , vol. 6, no. 2, pp. 251 - 256 , 1991.
- [20] Y. Zweiri, J. Whidborne and L. Seneviratne, "A mathematical transient model for the dynamics of a single cylinder diesel engine," in IET, York, 1998.
- [21] IEEE Std 1110-2002 Guide for Synchronous Generator Modeling Practices and Applications in Power System Stability Analyses, Nov. 2003.
- [22] O. W. S. D. S. Paul C. Krause, Analysis of Electric Machinery and Drive Systems, Wiley-IEEE Press, 2002.
- [23] Z. Guo and Deshang Sha, Xiaozhong Liao, "Voltage magnitude and frequency control of three-phase voltage source inverter for seamless transfer," Power Electronics, IET, vol. 7, no. 1, pp. 200-208, 2014.
- [24] N. Pogaku, and M. Prodanovic, T.C., Green, "Modeling, Analysis and Testing of Autonomous Operation of an Inverter-Based Microgrid," Power Electronics, IEEE Transactions on, vol. 22, no. 2, pp. 613-625, 2007.

- [25] R.E. Cosse, M.D. Alford, M., Hajiaghajani, E.R., Hamilton, "Turbine/generator governor droop/isochronous fundamentals - A graphical approach," in Petroleum and Chemical Industry Conference (PCIC), 2011, Toronto, ON, 2011.
- [26] P. Kundur, *Power System Stability and Control*, McGraw-Hill Professional, 1994.
- [27] M. Ehsani, Y. Gao, & A. Emadi. (2009). *Modern Electric, Hybrid Electric, and Fuel Cell Vehicles: Fundamentals, Theory, and Design*, Second Edition. CRC Press.
- [28] P.H., Bauer, Q.T., Bui, (2013). On the optimal choice of operating points in large series hybrids. *Electric Vehicle Symposium and Exhibition (EVS27)* (pp. 1-5). Barcelona: IEEE.
- [29] S. Overington, & S. Rajakaruna, (2014). "A novel model of internal combustion engine for high efficiency operation of hybrid electric vehicles and power systems." *Power Engineering Conference (AUPEC), 2014 Australasian Universities* , (pp. 1-6). Perth, WA.
- [30] Y. Wang, & L. Yongqi (2008). "An Oxygenating Additive for Reducing the Emission of Diesel Engine." *Bioinformatics and Biomedical Engineering, 2008. ICBBE 2008. The 2nd International Conference on* (pp. 3931 - 3933). Shanghai: IEEE.
- [31] Bedard, Roger, et al. *North American Ocean Energy Status – March 2007*. 2007. *Proceedings of the 7th European Wave and Tidal Energy Conference*. 11-13 September 2007. Porto, Portugal.
- [32] M. Mager, "HYDROKINETIC ENERGY (In-River, Tidal, and Ocean Current)," Alaska Center for Energy and Power, [Online]. Available: <http://energy-alaska.wikidot.com/hydrokinetic>. [Accessed 4 Jul 2015].
- [33] B. P. a. M. Previsic and C. G. H. a. R. Bedard, "System Level Design, Performance, Cost and Economic Assessment – Tacoma Narrows Washington Tidal In-Stream Power Plant," EPRI North American Tidal In Stream Power Feasibility Demonstration Project, Washington, 2006.
- [34] L. Lopes, Course notes of Elec 6461-Lecture 5: Modeling and control of single and three-phase PWM voltage source converters (VSCs), Concordia University, Montreal, 2013.
- [35] L. Lopes, Course notes of Elec 6461-Lecture 4: Closed loop control of dc-dc converters, Concordia University, Montreal, 2013.